

CERN-EP-2019-233
2020/05/19

CMS-SUS-19-009

Search for direct top squark pair production in events with one lepton, jets, and missing transverse momentum at 13 TeV with the CMS experiment

The CMS Collaboration*

Abstract

A search for direct top squark pair production is presented. The search is based on proton-proton collision data at a center-of-mass energy of 13 TeV recorded by the CMS experiment at the LHC during 2016, 2017, and 2018, corresponding to an integrated luminosity of 137 fb^{-1} . The search is carried out using events with a single isolated electron or muon, multiple jets, and large transverse momentum imbalance. The observed data are consistent with the expectations from standard model processes. Exclusions are set in the context of simplified top squark pair production models. Depending on the model, exclusion limits at 95% confidence level for top squark masses up to 1.2 TeV are set for a massless lightest supersymmetric particle, assumed to be the neutralino. For models with top squark masses of 1 TeV, neutralino masses up to 600 GeV are excluded.

"Published in the Journal of High Energy Physics as [doi:10.1007/JHEP05\(2020\)032](https://doi.org/10.1007/JHEP05(2020)032)."

1 Introduction

Supersymmetry (SUSY) [1–8] is an attractive extension of the standard model (SM), characterized by the presence of SUSY partners for every SM particle. These partner particles have the same quantum numbers as their SM counterparts, except for the spin, which differs by one-half unit. In models with R -parity conservation [9], the lightest supersymmetric particle (LSP) is stable, and, if neutral, could be a dark matter candidate [10]. The extended particle spectrum in SUSY scenarios allows for the cancellation of quadratic divergences arising from quantum corrections to the Higgs boson mass [11–15]. Scenarios realizing this cancellation often contain top squarks (\tilde{t}), SUSY partners of the SM top quark (t), and higgsinos, SUSY partners of the SM Higgs boson, with masses near the electroweak scale. The \tilde{t} pair production cross section is expected to be large compared to the electroweak production of higgsinos at CERN LHC for \tilde{t} masses near the electroweak scale.

In this paper, a search is presented for top squark pair production in final states with events from pp collisions at $\sqrt{s} = 13$ TeV, collected between 2016 and 2018 by the CMS experiment, corresponding to an integrated luminosity of 137 fb^{-1} . Two top squark decay modes are considered: the decay to a top quark and the lightest neutralino ($\tilde{\chi}_1^0$), which is taken to be the LSP, or the decay to a bottom quark (b) and the lightest chargino ($\tilde{\chi}_1^\pm$). In the latter scenario, it is assumed that the $\tilde{\chi}_1^\pm$ decays to a W boson and the $\tilde{\chi}_1^0$. The mass of the chargino is chosen to be $(m_{\tilde{t}} + m_{\tilde{\chi}_1^0})/2$. The corresponding diagrams are given in Fig. 1. The common experimental signature for pair production with these decay modes is $WW^{(*)} + bb + \tilde{\chi}_1^0\tilde{\chi}_1^0$. The analysis is based on events where one of the W bosons decays leptonically and the other hadronically. This results in the event selection of one isolated lepton, at least 2 jets, and large missing transverse momentum (p_T^{miss}) from the two neutralinos and the neutrino.

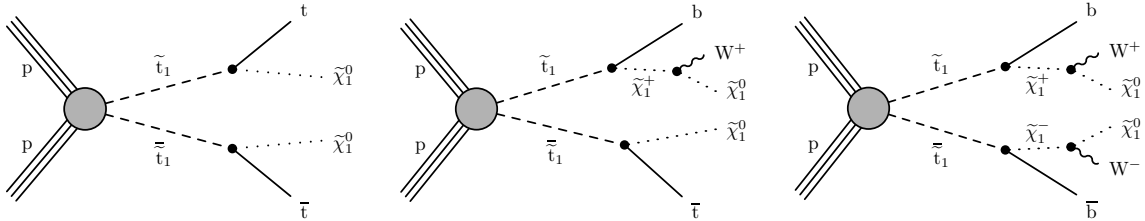


Figure 1: Diagrams for top squark pair production, with each \tilde{t} decaying either to $t\tilde{\chi}_1^0$ or to $b\tilde{\chi}_1^\pm$. For the latter decay, the $\tilde{\chi}_1^\pm$ decays further into a W boson and a $\tilde{\chi}_1^0$.

Dedicated searches for top squark pair production in 13 TeV proton-proton (pp) collision events have been carried out by both the ATLAS [16–25] and CMS [26–38] Collaborations. The search presented here improves the previous one [29] by adding the data collected in 2017 and 2018, resulting in approximately a factor of four increase in the size of the data sample. In addition, new search regions have been added, which are sensitive to scenarios where the mass of the top squark is close to the sum of the masses of either the $\tilde{\chi}_1^0$ and the top quark, or the $\tilde{\chi}_1^0$ and the W boson. These scenarios are referred to as compressed mass scenarios hereafter. In addition, a method has been implemented to identify top quarks that decay hadronically, and also the background estimation techniques have been improved. The paper is organized as follows: Section 2 and 3 describe the CMS detector and the simulated samples used in this analysis. The object reconstruction and search strategy are presented in Section 4. The background prediction methods are described in Section 5, and the relevant systematic uncertainties are discussed in Section 6. Results and interpretations are detailed in Section 7, and a summary is presented in Section 8.

2 The CMS detector

The central feature of the CMS apparatus is a superconducting solenoid of 6 m internal diameter, providing a magnetic field of 3.8 T. Within the solenoid volume are a silicon pixel and strip tracker, a lead tungstate crystal electromagnetic calorimeter (ECAL), and a brass and scintillator hadron calorimeter (HCAL), each composed of a barrel and two endcap sections. Forward calorimeters extend the pseudorapidity (η) coverage provided by the barrel and endcap detectors. Muons are detected in gas-ionization chambers embedded in the steel flux-return yoke outside the solenoid.

Events of interest are selected using a two-tier trigger system. The first level, composed of custom hardware processors, uses information from the calorimeters and muon detectors to select events in a fixed time interval of less than $4\ \mu\text{s}$. The second level, called the high-level trigger, further decreases the event rate from around 100 kHz to less than 1 kHz before data storage. A more detailed description of the CMS detector, together with a definition of the coordinate system used and the relevant kinematic variables, can be found in Refs. [39, 40]. The pixel tracker was upgraded before the start of the data taking period in 2017, providing one additional layer of measurements compared to the older tracker [41].

3 Simulated samples

Monte Carlo (MC) simulation is used to design the search, to aid in the estimation of SM backgrounds, and to evaluate the sensitivity of the analysis to top squark pair production. Samples of events of SM $t\bar{t}$, $W + \text{jets}$, $Z + \text{jets}$, and $\gamma + \text{jets}$ processes and simplified SUSY top squark pair production models are generated at leading-order (LO) in quantum chromodynamics (QCD) using the MADGRAPH5_aMC@NLO 2 (2.2.2 or 2.4.2) generator [42]. The MADGRAPH5_aMC@NLO at next-to-LO (NLO) in QCD is used to generate samples of $t\bar{t}Z$, WZ , and $t\bar{t}W$ events, while single top quark events are generated at NLO in QCD using the POWHEG 2.0 [43–46] program. Samples of $W + \text{jets}$, $t\bar{t}$, and SUSY events are generated with four, three, and two additional partons included in the matrix element calculations, respectively.

Since the data used for this search were collected in three distinct periods (2016, 2017, and 2018), different detector MC simulations are used to reflect the running conditions. In addition, in some cases, the generator settings are also different as described below.

The NNPDF3.0 [47, 48] parton distribution functions (PDFs) are used to generate all 2016 MC samples, while NNPDF3.1 [49] is used for 2017 and 2018 samples. The parton shower and hadronization are modeled with PYTHIA 8.2 (8.205 or 8.230) [50]. The MLM [51] and FxFx [52] prescriptions are employed to match partons from the matrix element calculation to those from the parton showers, for the LO and NLO samples, respectively.

The 2016 MC samples are generated with the CUETP8M1 [53] PYTHIA tune. For the later running periods, the CP5 [54] tune was used for SM samples, and the SUSY samples use LO PDFs, combined with tune CP2, in order to avoid large negative weights that arise from PDF interpolations at very large energies. The differences in jet kinematic properties between the SUSY and SM samples are due to different PYTHIA tunes and are within 5% of each other. The GEANT4 [55] package is used to simulate the response of the CMS detector for all SM processes, while the CMS fast simulation program [56, 57] is used for SUSY samples.

Cross section calculations performed at next-to-NLO (NNLO) in QCD are used to normalize the MC samples of $W + \text{jets}$ [58] and single top quark [59, 60] events. The $t\bar{t}$ samples are nor-

malized to a cross section determined at NNLO in QCD that includes the resummation of the next-to-next-to-leading logarithmic (NNLL) soft-gluon terms [61–67]. Monte Carlo samples of other SM background processes are normalized to cross sections obtained from the MC event generators at either LO or NLO in QCD. The SUSY cross sections are computed at approximately NNLO plus NNLL precision with all other SUSY particles assumed to be heavy and decoupled [68–74].

To improve the modeling of the multiplicity of additional jets either from initial-state radiation (ISR) or final-state radiation (FSR), simulated SM and SUSY events are reweighted so as to make the jet multiplicity agree with data. The reweighting is applied to all SUSY samples but only to 2016 SM samples. No reweighting is applied for 2017 and 2018 SM simulation because of the improved tuning of the MC generators mentioned above. The procedure is based on a comparison of the light-flavor jet multiplicity in dilepton $t\bar{t}$ events in data and simulation. The comparison is performed after selecting events with two leptons and two b-tagged jets, which are jets identified as originating from the fragmentation of bottom quarks. The reweighting factors obtained vary from 0.92 to 0.51 for one to six additional jets. The uncertainties in the reweighting factors are evaluated as half of the deviation from unity. These uncertainties cover the data-simulation differences observed in $t\bar{t}$ enriched validation samples obtained by selecting events with an $e\mu$ pair and at least one b-tagged jet.

The p_T^{miss} and its vector (\vec{p}_T^{miss}), defined in Section 4, are key ingredients of the analysis. The modeling of their resolution in the simulation is studied in $\gamma + \text{jets}$ samples for each data taking period. Based on these studies, the simulated p_T^{miss} resolution is corrected with scale factors, the magnitudes of which are around 10% for the 2018 data and up to 15% for the latter subset of the 2017 data. The correction factors for the earlier subset of the 2017 data, or the entire 2016 data are close to unity. The variations seen in the p_T^{miss} resolution factors in the three data taking periods are mainly caused by different pileup and detector conditions, which are addressed in the next section.

4 Event reconstruction and search strategy

The overall strategy of the analysis follows that of the search presented in Ref. [29]. Three categories of search regions are defined. The “standard selection” is designed to be sensitive to the majority of the top squark scenarios under consideration with $\Delta m(\tilde{t}, \tilde{\chi}_1^0) > m_t$. In this paper we use the symbol $\Delta m(a, b)$ to indicate the mass difference between particles a and b, and m_a to denote the mass of a. Two additional sets of signal regions are used to target decays of the top squark to a top quark and a neutralino with mass splittings between these particles of either $\Delta m(\tilde{t}, \tilde{\chi}_1^0) \sim m_t$, or $\Delta m(\tilde{t}, \tilde{\chi}_1^0) \sim m_W$.

4.1 Event reconstruction

The events used in this analysis are selected using triggers that require either large p_T^{miss} , or the presence of an isolated electron or muon. The \vec{p}_T^{miss} is first computed from the negative vector sum of the p_T of all particle-flow candidates, described below. The trigger selects events with $p_T^{\text{miss}} > 120$ GeV. The minimum requirement on the lepton p_T varied between 27 and 35 GeV for electrons, and between 24 and 27 GeV for muons, depending on the data taking period. The combined trigger efficiency, measured with a data sample of events with a large scalar sum of jet p_T , is greater than 99% for events with $p_T^{\text{miss}} > 250$ GeV and lepton $p_T > 20$ GeV.

The CMS event reconstruction is based on a particle-flow (PF) algorithm [75]. The algorithm combines information from all CMS subdetectors to identify charged and neutral hadrons, pho-

tons, electrons, and muons, collectively referred to as PF candidates.

Each event must contain at least one reconstructed pp interaction vertex. The reconstructed vertex with the largest value of the summed p_T^2 of physics objects is taken to be the primary vertex (PV). The physics objects are the objects reconstructed by the anti- k_T jet finding algorithm [76–78] with the tracks assigned to the vertex as inputs, and the associated missing transverse momentum (H_T^{miss}), taken as the magnitude of the negative vector sum of the p_T of those jets.

Events with possible contributions from beam halo interactions or anomalous noise in the calorimeter are rejected using dedicated filters [79]. For the 2017 and 2018 data taking periods, the ratio of the scalar sums of jet p_T within $|\eta| < 5.0$ and of jet p_T within $|\eta| < 2.4$ is required to be smaller than 1.5 to reject events with significant p_T^{miss} arising from noise in the ECAL endcap forward region. Additionally, during part of the 2018 data taking period, two sectors of the HCAL endcap detector experienced a power loss. The affected data sample size is about 39 fb^{-1} . As the identification of both electrons and jets depends on correct energy fraction measurements, events from the affected data taking periods containing an electron or a jet in the region $-2.4 < \eta < -1.4$ and azimuthal angle $-1.6 < \phi < -0.8$ radians are rejected. The effect is estimated to be an approximately 2% loss in signal and background acceptance for the full dataset. The simulation is corrected to take this loss into account.

After these initial requirements, we apply an event preselection summarized in Table 1 and described below. Selected events are required to have exactly one electron [80] or muon [81] originating from the PV and isolated from other activity in the event. Leptons are identified as isolated if the scalar sum of the p_T of all PF candidates in a cone around the lepton, excluding the lepton itself, is less than 10% of the lepton p_T . Typical lepton selection efficiencies are approximately 85% for electrons and 95% for muons, depending on p_T and η .

The PF candidates are clustered into jets using the anti- k_T algorithm with a distance parameter of 0.4. Jet energies are corrected for contributions from multiple interactions in the same or adjacent beam crossing (pileup) [82, 83] and to account for nonuniformity in the detector response. These jet energy corrections are propagated to the calculation of \vec{p}_T^{miss} [84, 85].

Jets in the analysis are required to be within $p_T > 30 \text{ GeV}$ and $|\eta| < 2.4$, and the number of these jets (N_j) is required to be at least two. Jets overlapping with the selected lepton within a cone radius of $\Delta R = 0.4$ are not counted. The distribution of the number of jets after the preselection requirements is shown in Fig. 2 (upper right). The jet multiplicity is used to define the signal region bins to optimize sensitivity for a variety of signal models and SUSY particle masses, as shown in this figure.

After these requirements, jets originating from a bottom quark fragmentation are identified as b-tagged jets by the combined secondary vertex algorithm using a deep neural network (DeepCSV) [86]. The preselection requires at least one b-tagged jet with either a medium or tight working point. The threshold on the discriminator value corresponding to the medium (tight) working point is chosen so that the tagging rate for light-flavor jets is about 1% (0.1%), corresponding to an efficiency to identify a jet originating from a bottom-flavored hadron of 65–80 (40–65)%, for jet p_T of 30–400 GeV.

To enhance sensitivity to signal scenarios with a compressed mass spectra, we use a secondary vertex (SV), not associated to jets or leptons, to identify soft b hadrons [30] with $p_T > 1 \text{ GeV}$ and $|\eta| < 2.5$. The SV is reconstructed by the inclusive vertex finding algorithm [87]. At least two tracks must be associated to the SV and the sum of the transverse momenta of all the associated tracks is required to be below 20 GeV. The distance between the SV and the PV must

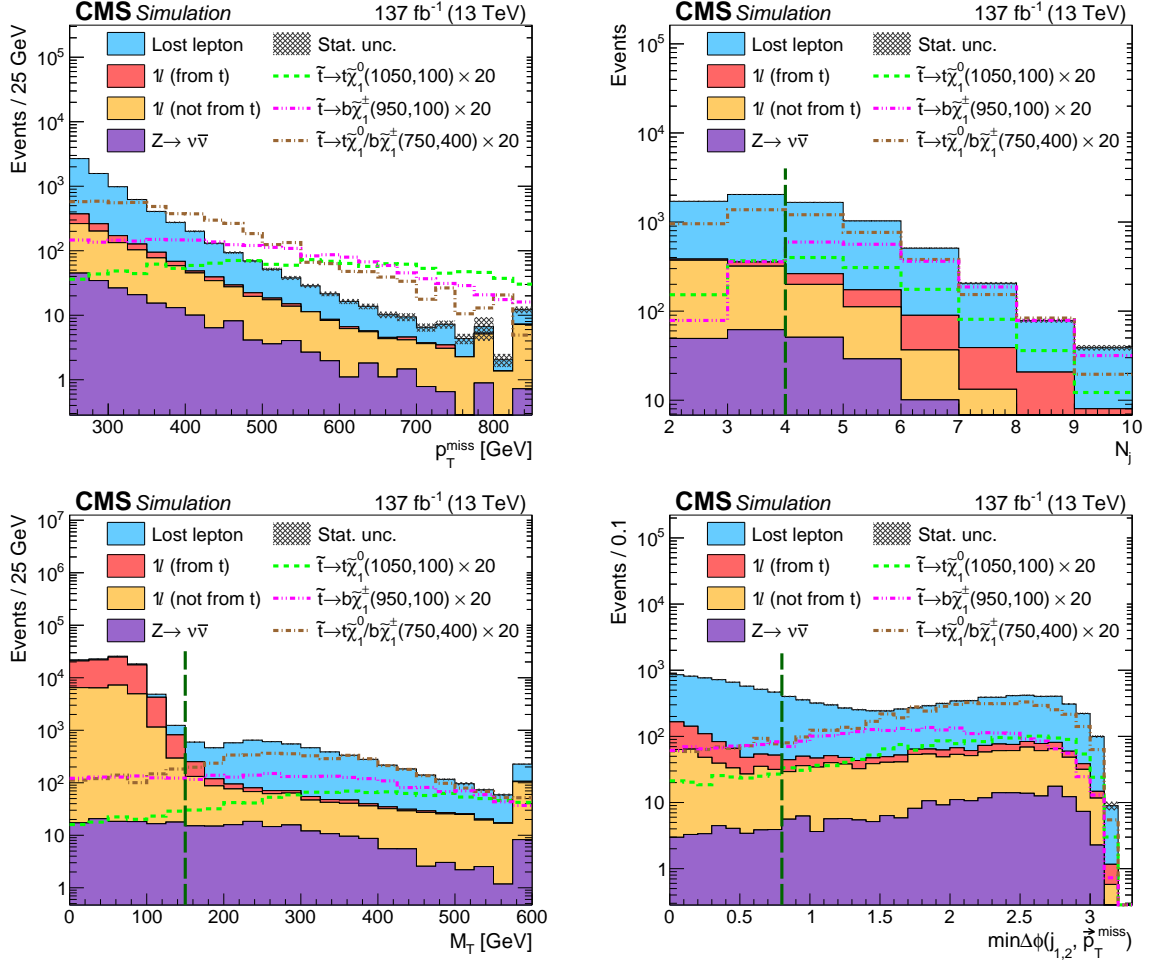


Figure 2: The distributions of p_T^{miss} (upper left) and N_j (upper right) are shown after applying the preselection requirements of Table 1, including the requirement on the variable shown, and the distributions of M_T (lower left) and $\min \Delta \phi(j_{1,2}, \vec{p}_T^{\text{miss}})$ (lower right) are shown after applying the preselection requirements, excluding the requirement on the variable shown with the green, dashed vertical line marking the location of the requirement. The stacked histograms for the SM background contributions (categorized as described in Section 5) are from the simulation to illustrate the discriminating power of these variables. The gray hashed region indicates the statistical uncertainty of the simulated samples. The last bin in each distribution includes the overflow events. The expectations for three signal hypotheses are overlaid, and the corresponding numbers in parentheses in the legends refer to the masses of the top squark and neutralino, respectively. For models with $b\tilde{\chi}_1^\pm$ decays, the mass of the chargino is chosen to be $(m_{\tilde{t}} + m_{\tilde{\chi}_1^0})/2$.

Table 1: Summary of the event preselection requirements. The magnitude of the negative vector sum of the p_T of all jets and leptons in the event is denoted by H_T^{miss} . The symbols p_T^ℓ and η^ℓ correspond to the transverse momentum and pseudorapidity of the lepton. The symbol p_T^{sum} is the scalar sum of the p_T of all (charged) PF candidates in a cone around the lepton (track), excluding the lepton (track) itself. Finally, $N_{b, \text{med}}$ and $N_{b, \text{soft}}$ are the multiplicity of b-tagged jets (medium working point) and soft b objects, respectively.

Trigger (2016)	$p_T^{\text{miss}} > 170 \text{ GeV}$ or $p_T^{\text{miss}} > 120 \text{ GeV}$ and $H_T^{\text{miss}} > 120 \text{ GeV}$ or isolated $\mu(e)$ with $p_T^\ell > 24(25) \text{ GeV}$
Trigger (2017, 2018)	$p_T^{\text{miss}} > 120 \text{ GeV}$ and $H_T^{\text{miss}} > 120 \text{ GeV}$ or isolated $\mu(e)$ with $p_T^\ell > 27(35) \text{ GeV}$
p_T^{sum} cone size	for μ or e : $\Delta R = \min[\max(0.05, 10 \text{ GeV}/p_T^\ell), 0.2]$ for track: $\Delta R = 0.3$
Lepton	$\mu(e)$ with $p_T^\ell > 20 \text{ GeV}$, $ \eta^\ell < 2.4$ (1.44) $p_T^{\text{sum}} < 0.1 \times p_T^\ell$
Veto lepton	μ or e with $p_T^\ell > 5 \text{ GeV}$, $ \eta^\ell < 2.4$ $p_T^{\text{sum}} < 0.2 \times p_T^\ell$
Veto track	Charged PF candidate, $p_T > 10 \text{ GeV}$, $ \eta < 2.4$ $p_T^{\text{sum}} < \min(0.1 \times p_T, 6 \text{ GeV})$
Jets	$p_T > 30 \text{ GeV}$, $ \eta < 2.4$, $N_j \geq 2$
b tagging	$N_{b, \text{med}} \geq 1$ for standard and $\Delta m(\tilde{t}, \tilde{\chi}_1^0) \sim m_t$ selection $N_{b, \text{soft}} \geq 1$ for $\Delta m(\tilde{t}, \tilde{\chi}_1^0) \sim m_W$ selection
p_T^{miss}	$> 250 \text{ GeV}$
M_T	$> 150 \text{ GeV}$
$\min \Delta\phi(j_{1,2}, \vec{p}_T^{\text{miss}})$	> 0.8 radians for standard search > 0.5 radians for compressed scenarios

be <3 cm and the significance of this distance is required to be >4 . The cosine of the pointing angle defined by the scalar product between the distance vector, $\overrightarrow{(PV,SV)}$, and the \vec{p}_{SV} , where the \vec{p}_{SV} is the total three-momentum of the tracks associated with the SV, must be >0.98 . These requirements help suppress background from light-flavor hadrons and jets. Events containing objects that pass these selections, are said to contain a “soft b object”. These requirements result in a 40–55 (2–5)% efficiency to select a soft b object originating from a soft bottom-flavor (light-flavor) hadron. As listed in Table 1, the preselection requires the presence of at least one soft b object in the signal regions dedicated to the compressed mass spectra.

The background processes relevant for this search are semileptonic or dileptonic $t\bar{t}$ ($t\bar{t} \rightarrow 1\ell + X$ or $t\bar{t} \rightarrow 2\ell + X$), single top quark production (mostly in the tW channel), $W + \text{jets}$, and processes containing a Z boson decaying into a pair of neutrinos ($Z \rightarrow \nu\bar{\nu}$), such as $t\bar{t}Z$ or WZ . Contributions to the background from semileptonic $t\bar{t}$ and $W + \text{jets}$ are heavily suppressed by requiring in the preselection that the transverse mass (M_T) be greater than 150 GeV and the p_T^{miss} to be greater than 250 GeV, as shown in Fig. 2 (upper left and lower left, respectively). The M_T is defined as $\sqrt{2p_T^\ell p_T^{\text{miss}}[1 - \cos(\Delta\phi)]}$ with p_T^ℓ denoting the lepton p_T , and $\Delta\phi$ the azimuthal separation between the lepton direction and \vec{p}_T^{miss} .

In addition, to suppress background from processes with two leptonically decaying W bosons, primarily $t\bar{t}$ and tW , we also reject events containing either an additional lepton passing a loose selection (denoted as “veto lepton” in Table 1) or an isolated track. Further rejection is achieved by requiring that the minimum angle in the transverse plane between the \vec{p}_T^{miss} and the directions of the two leading p_T jets in the event (denoted as $j_{1,2}$), $\min \Delta\phi(j_{1,2}, \vec{p}_T^{\text{miss}})$, is greater than 0.8 or 0.5, depending on the signal region. This can be seen from the distribution of $\min \Delta\phi(j_{1,2}, \vec{p}_T^{\text{miss}})$, after applying the rest of the preselection requirements, shown in Fig. 2 (lower right).

In addition to the preselection requirements, we also use two deep neural networks (DNNs) to categorize events based on the identification of hadronically decaying top quarks.

One DNN, referred to as the resolved tagger, uses the DeepResolved algorithm to identify hadronically decaying top quarks with a moderate Lorentz boost. The decay products of these objects result in three separate jets (resolved top quark decay). The DeepResolved algorithm identifies top quarks decaying into three distinct jets passing the selection requirements. The three jets ($p_T > 40, 30, 20$ GeV) of each candidate must have an invariant mass between 100 and 250 GeV, no more than one of the jets can be identified as a b-tagged jet, and the three jets must all lie within a cone of $\Delta R < 3.14$ of the trijet centroid.

A neural network is used to distinguish trijet combinations which match to a top quark versus those which do not. The network uses high-level information such as the invariant mass of the trijet system and of the individual dijet pairs, as well as kinematic information from each jet. This includes its Lorentz vector, DeepCSV heavy-flavor discriminator values, jet shape variables, and detector level particle multiplicity and energy fraction variables. The network is trained using both $t\bar{t}$ and QCD simulation, and data as training inputs. The simulation is used to define the examples of signal and background. The signal is defined as any trijet passing the preselection requirements, where each jet is matched to a generator level daughter of a top quark within a cone of $\Delta R < 0.4$ and the overall trijet system is matched to the generator level top quark within a cone of $\Delta R < 0.6$. The background category is defined as any trijet combination that is not categorized as signal. This includes trijet combinations for which some, but not all, of the jets match top decay products. The data is included in the training to inhibit the network from learning features of the MC which are not present in data. This is achieved

through a technique called domain adaption via gradient reversal [88]. With this method, an additional output is added to the neural network to distinguishing between trijet candidates from QCD simulation and a QCD-enriched data sample. The main network is then restricted to minimize its ability to discriminate simulation from data. This yields a network with good separation between signal and background while minimizing over-fitting on features that exist only in simulation. Before the final selection of trijets as top quarks can be made, any trijet candidates that may share the jets with another candidate must be removed. This is achieved by always favoring the candidate with a higher top discriminator value as determined by the neural network. The reconstructed candidates are identified as hadronic tops when the neural network discriminator is above the threshold corresponding to an efficiency of 45% and the mistagging rate is 10% for dileptonic $t\bar{t}$ events.

The second DNN, referred to as a merged tagger, uses the DeepAK8 [89] algorithm to identify top quarks with large boost, where the decay products are merged into a single jet (merged top quark decay). The identification of this boosted top quark signature is based on anti- k_T jets clustered with a distance parameter of 0.8. The efficiency for lepton + hadronic-top events is 40% and the mistagging rate is 5% for dileptonic $t\bar{t}$ events.

4.2 Search strategy

The signal regions for the standard search are summarized in Table 2, and are defined by categorizing events passing the preselection requirements based on N_j , the number of identified hadronic top quarks, p_T^{miss} , the invariant mass ($M_{\ell b}$) of the lepton and the closest b-tagged jet in ΔR , and a modified version of the topness variable [90], t_{mod} [27], which is defined as:

$$t_{\text{mod}} = \ln(\min S), \text{ with } S = \frac{\left(m_W^2 - (p_\nu + p_\ell)^2\right)^2}{a_W^4} + \frac{\left(m_t^2 - (p_b + p_W)^2\right)^2}{a_t^4},$$

with resolution parameters $a_W = 5 \text{ GeV}$ and $a_t = 15 \text{ GeV}$. The t_{mod} variable is a χ^2 -like variable that discriminates signal from leptonically decaying $t\bar{t}$ events: an event with a small value of t_{mod} is likely to be a dilepton $t\bar{t}$ event, while signal events tend to have larger t_{mod} values. The first term in its definition corresponds to the top quark decay containing the reconstructed lepton, and the second term corresponds to the top quark decay containing the missing lepton. The p_W in the second term symbolizes the momentum of the missing lepton and neutrino from the W decay. The minimization of the variable S is done with respect to all components of the three momentum \vec{p}_W and the component of the three momentum \vec{p}_ν along the beam line with the constraints that $\vec{p}_T^{\text{miss}} = \vec{p}_{T,W} + \vec{p}_{T,\nu}$ and $p_W^2 = m_W^2$. The distribution of t_{mod} for events passing the preselection is shown in Fig. 3 (upper left). The t_{mod} distribution is split into three bins, each sensitive to a different mass splitting of the top squark and neutralino.

In events containing a leptonically decaying top quark, the invariant mass of the lepton and the bottom quark jet from the same top quark decay is bound by

$$M_{\ell b} \leq m_t \sqrt{1 - \frac{m_W^2}{m_t^2}}.$$

This bound does not apply to either W + jets events or signal events, where the top squark decays to a bottom quark and a chargino. To maintain acceptance to a broad range of signal scenarios, rather than requiring a selection on $M_{\ell b}$, events are placed into low- or high- $M_{\ell b}$ categories if the value of $M_{\ell b}$ is less or greater than 175 GeV, respectively. In signal regions

Table 2: The 39 signal regions of the standard selection, with each neighboring pair of values in the p_T^{miss} bins column defines a single signal region. At least one b-tagged jet selected using the medium (tight) working point is required for search regions with $M_{\ell b}$ lower (higher) than 175 GeV. For the top quark tagging categories, we use the abbreviations U for untagged, M for merged, and R for resolved.

Label	N_j	t_{mod}	$M_{\ell b}$ [GeV]	t tagging category	p_T^{miss} bins [GeV]
A0				—	[600, 750, $+\infty$]
A1	2–3	>10	≤ 175	U	[350, 450, 600]
A2				M	[250, 600]
B	2–3	>10	>175	—	[250, 450, 700, $+\infty$]
C	≥ 4	≤ 0	≤ 175	—	[350, 450, 550, 650, 800, $+\infty$]
D	≥ 4	≤ 0	>175	—	[250, 350, 450, 600, $+\infty$]
E0				—	[450, 600, $+\infty$]
E1	≥ 4	0–10	≤ 175	U	[250, 350, 450]
E2				M	[250, 350, 450]
E3				R	[250, 350, 450]
F	≥ 4	0–10	>175	—	[250, 350, 450, $+\infty$]
G0				—	[450, 550, 750, $+\infty$]
G1	≥ 4	>10	≤ 175	U	[250, 350, 450]
G2				M	[250, 350, 450]
G3				R	[250, 350, 450]
H	≥ 4	>10	>175	—	[250, 500, $+\infty$]

with $M_{\ell b} > 175$ GeV, at least one jet is required to satisfy the tight b tagging working point of the DeepCSV discriminator to suppress the background from $W + \text{jets}$ events. The distribution of $M_{\ell b}$ in the signal regions is shown in Fig. 3 (upper right). As seen from this figure, the low $M_{\ell b}$ regions are more sensitive to $t\tilde{\chi}_1^0$ and the $M_{\ell b} > 175$ GeV are more sensitive to $b\tilde{\chi}_1^\pm$.

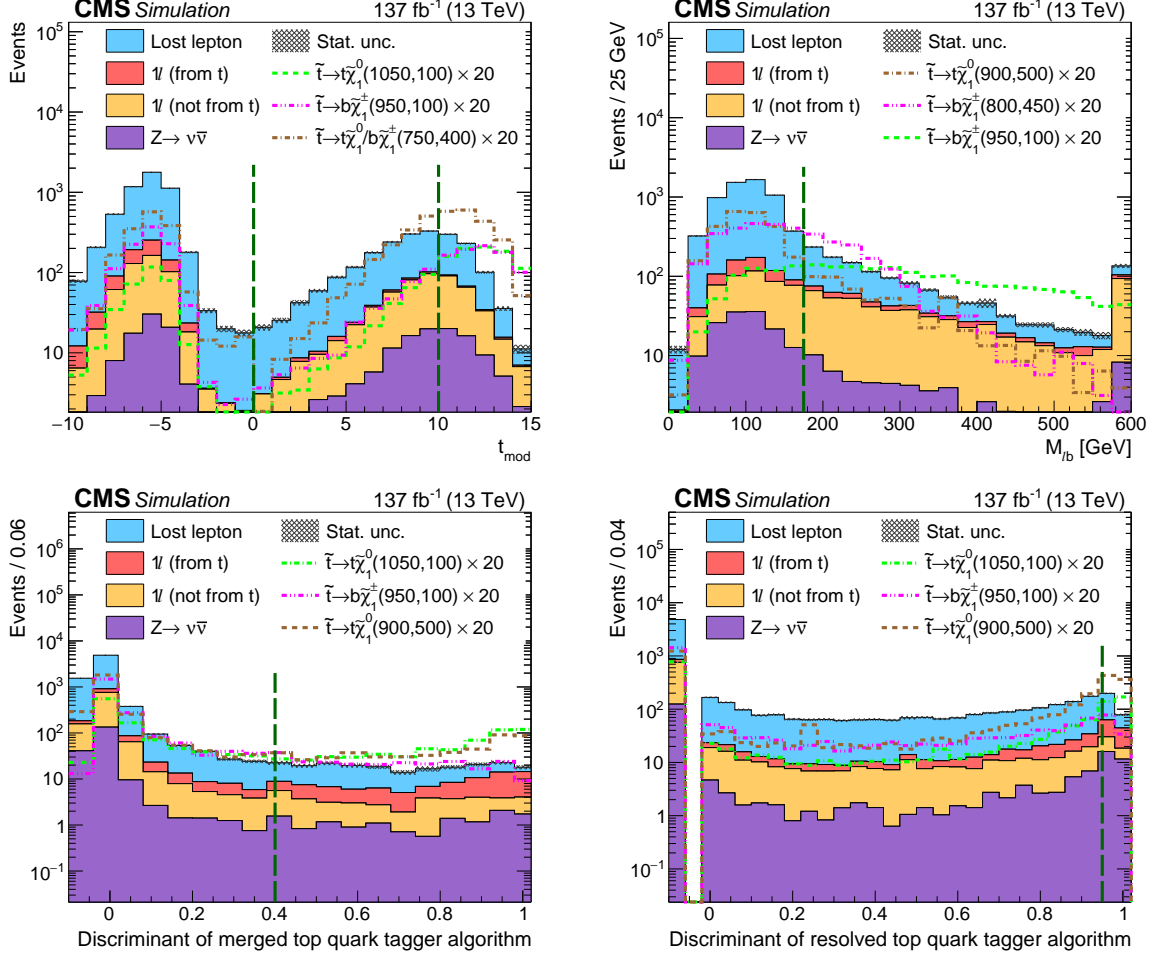


Figure 3: The distributions of t_{mod} (upper left), $M_{\ell b}$ (upper right), the merged top quark tagging discriminant (lower left), and the resolved top quark tagging discriminant (lower right) are shown after the preselection requirements. The green, dashed vertical lines mark the locations of the binning or tagging requirements. The stacked histograms showing the SM background contributions (categorized as described in Section 5) are from the simulation to illustrate the discriminating power of these variables. The gray hashed region indicates the statistical uncertainty of the simulated samples. Events outside the range of the distributions shown are included in the first or last bins. The expectations for three signal hypotheses are overlaid, and the corresponding numbers in parentheses in the legends refer to the masses of the top squark and neutralino, respectively. For models with $b\tilde{\chi}_1^\pm$ decays, the mass of the chargino is chosen to be $(m_{\tilde{t}} + m_{\tilde{\chi}_1^0})/2$.

Hadronic top quark taggers are used in signal regions sensitive to SUSY scenarios with hadronically decaying top quarks when most of the expected SM background does not contain such a top quark decay. Therefore, the hadronic top taggers are deployed in the low $M_{\ell b}$, $t_{\text{mod}} \geq 0$, and relatively modest $p_{\text{T}}^{\text{miss}}$ signal regions. Events containing two or three jets and $p_{\text{T}}^{\text{miss}} \leq 600$ GeV, or at least four jets and $p_{\text{T}}^{\text{miss}} \leq 450$ GeV, are categorized according to the presence of a

merged top quark tag. The resolved top quark tagger is used to further categorize events with four or more jets. If an event contains both merged and resolved top quark tags, it is placed in the *merged* top category, while events containing neither are categorized as *untagged*. Distributions of the discriminant of the merged and resolved top quark taggers in the signal regions are also shown in Fig. 3 (lower left and lower right, respectively).

The small mass splitting in SUSY models with a compressed mass spectrum results in soft decay products. High values of p_T^{miss} can only be caused by large boost from ISR. As a result, in signal regions targeting these models the jet with the highest p_T is expected to be from ISR and therefore it is required to not be identified as a bottom quark jet. We also impose an upper bound on the lepton p_T relative to the p_T^{miss} , since this requirement provides an additional handle to reject SM $W + \text{jets}$ and $t\bar{t}$ backgrounds. Regions targeting signal scenarios with $\Delta m(\tilde{t}, \tilde{\chi}_1^0) \sim m_t$ require at least five jets and at least one b-tagged jet based on the DeepCSV medium working point. For signal scenarios with $\Delta m(\tilde{t}, \tilde{\chi}_1^0) \sim m_W$, the bottom quarks are expected to have low p_T . Therefore, in these regions the N_j selection is relaxed to $N_j \geq 3$ and instead of requiring the presence of a b-tagged jet we require the presence of a soft b object. Note that soft b objects are included in the jet count in these regions. The requirements for the two sets of signal regions targeting compressed mass spectrum SUSY scenarios are summarized in Table 3.

Table 3: Definitions of the total 10 search regions targeting signal scenarios with a compressed mass spectrum. Search regions for $\Delta m(\tilde{t}, \tilde{\chi}_1^0) \sim m_t$ and $\sim m_W$ scenarios are labeled with the letter I and J, respectively. The symbol p_T^ℓ denotes the transverse momentum of the lepton. Each neighboring pair of values in the p_T^{miss} bins column defines a single signal region.

Compressed spectra with $\Delta m(\tilde{t}, \tilde{\chi}_1^0) \sim m_t$		
Label I	Selection criteria	$N_j \geq 5$, leading- p_T jet not b-tagged, $N_{\text{b, med}} \geq 1$, $p_T^\ell < \max(50, 250 - 100 \times \Delta\phi(\vec{p}_T^{\text{miss}}, \vec{p}_T^\ell))$ GeV,
	p_T^{miss} bins [GeV]	[250, 350, 450, 550, 750, $+\infty$]
Compressed spectra with $\Delta m(\tilde{t}, \tilde{\chi}_1^0) \sim m_W$		
Label J	Selection criteria	$N_j \geq 3$, leading- p_T jet not b-tagged, $N_{\text{b, soft}} \geq 1$, $p_T^\ell < \max(50, 250 - 100 \times \Delta\phi(\vec{p}_T^{\text{miss}}, \vec{p}_T^\ell))$ GeV,
	p_T^{miss} bins [GeV]	[250, 350, 450, 550, 750, $+\infty$]

5 Background estimation

Three categories of SM backgrounds remain after the selection requirements described in Section 4.

- The lost-lepton background consists of events with two W bosons decaying leptonically, where one of the leptons is either not reconstructed, or not identified. This background arises primarily from $t\bar{t}$ events, with a smaller contribution from single top quark processes. It is the dominant background in regions with low values of $M_{\ell b}$, no top quark tag, or $N_j \geq 5$. This background is estimated using a dilepton control sample.

- The one-lepton background consists of events with a single W boson decaying leptonically and without any additional source of genuine p_T^{miss} . The requirements of $p_T^{\text{miss}} > 250 \text{ GeV}$ and $M_T > 150 \text{ GeV}$ heavily suppress this background. The one-lepton background is estimated from simulation when it originates from top quark decays (mainly semi-leptonic $t\bar{t}$). Background events not originating from top quark decays, instead mainly from direct W production, are estimated using a control sample of events with no b-tagged jets.
- The $Z \rightarrow \nu\bar{\nu}$ background consists of events with a single leptonically decaying W boson and a Z boson that decays to a pair of neutrinos, i.e., $pp \rightarrow t\bar{t}Z$ or WZ . This background is estimated using simulation.

5.1 Lost-lepton background

The lost-lepton background in each of the signal regions is estimated from corresponding dilepton control samples. Each dilepton control sample is obtained with the signal selections except for the requirement of a second isolated lepton with $p_T > 10 \text{ GeV}$ and the removal of the lepton, track, and tau vetoes. The estimated background in each search region is obtained from the yield of data events in the corresponding control sample and a transfer factor obtained from simulation, $R_{\text{MC}}^{\text{lost-}\ell/2\ell}$. The transfer factor is defined as the ratio of the expected lost-lepton yield in the signal region and the yield of dilepton SM events in the control sample. These transfer factors are validated by checking the modeling of lepton reconstruction and selections as well as the kinematical properties of leptons in simulation. Corrections obtained from studies of samples of $Z, J/\psi \rightarrow \ell\ell$ events are applied to the transfer factor to account for differences in lepton reconstruction and selection efficiencies between data and simulation. The kinematical properties of leptons are well modeled in simulation and have a data to simulation agreement within 10% or better. Simulation shows that the dilepton control sample have high purity (70–80%) of the main processes (dileptonic $t\bar{t}$ and tW) contributing to the lost-lepton background. Small contamination from semileptonic $t\bar{t}$ and other process, where the additional lepton is a fake or non-prompt lepton, are subtracted from the control sample data yields.

When defining the p_T^{miss} in this control sample, the trailing lepton \vec{p}_T is added to \vec{p}_T^{miss} to enhanced data statistics and all \vec{p}_T^{miss} related quantities are recalculated. The distribution of p_T^{miss} for after this addition is shown in Fig. 4 (left) for an inclusive selection.

Some control samples only contain a small number of events. These samples, corresponding to multiple p_T^{miss} bins, are combined into a single control sample until the expected yield in simulation is at least five events, as detailed in Table 4. The number of data events in the combined control sample is used to estimate the sum of expected background events in the corresponding signal regions. This sum is then distributed across p_T^{miss} bins according to the expectation from simulation using an extrapolation factor $k(p_T^{\text{miss}})$. Additional corrections to account for the p_T^{miss} shape mismodeling observed in simulation with respect to data are derived in an orthogonal $t\bar{t}$ enriched dilepton sample and applied to the simulation in these regions.

The lost-lepton background in each signal region, $N_{\text{lost-}\ell}^{\text{SR}}$, is obtained by scaling the number of events in the control sample, $N_{2\ell}^{\text{CR}}$, using the transfer factor $R_{\text{MC}}^{\text{lost-}\ell/2\ell}$ and the p_T^{miss} extrapolation factor $k(p_T^{\text{miss}})$ as follows:

$$N_{\text{lost-}\ell}^{\text{SR}} = N_{2\ell}^{\text{CR}} R_{\text{MC}}^{\text{lost-}\ell/2\ell} k(p_T^{\text{miss}}). \quad (1)$$

The dominant uncertainties in the transfer factors are the statistical uncertainties in the simulated samples, the uncertainties in the lepton efficiencies, and the uncertainties in the jet energy scale. These uncertainties range between 3–68%, 2–20%, and 1–16%, respectively. Uncertainties

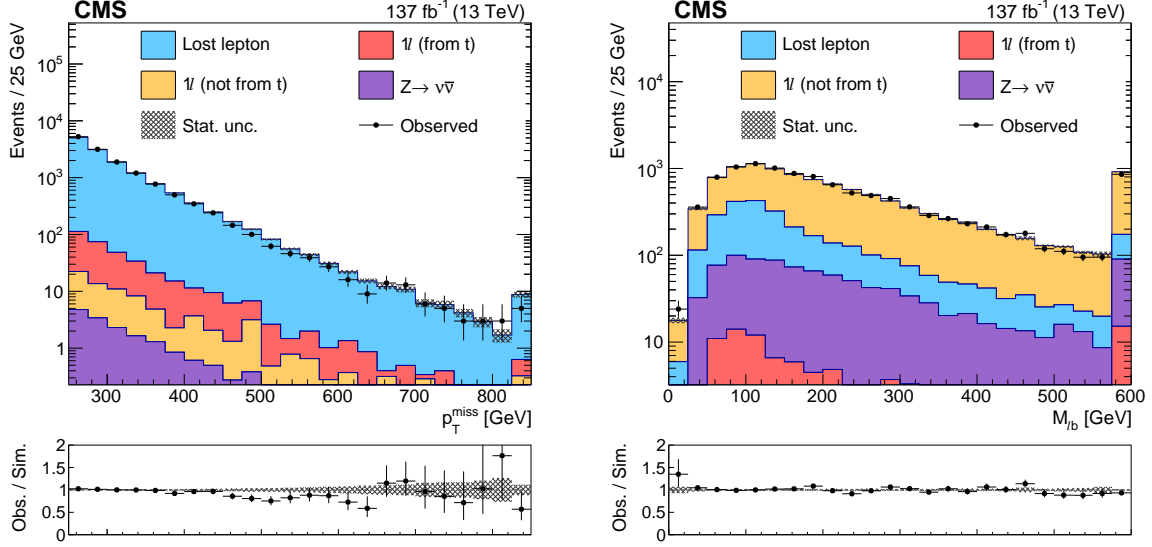


Figure 4: Distributions of kinematic variables in the inclusive control samples used for the background estimation. The gray hashed region indicates the statistical uncertainty of the simulated samples. The distributions for data are shown as points with error bars corresponding to the statistical uncertainty. The stacked histograms show the expected SM background contributions from simulation, normalized to the number of events observed in data. The last bin in each distribution also includes the overflow. Left: Distribution of p_T^{miss} in the dilepton control sample. Right: Distribution of $M_{\ell b}$ in the $0\ell b$ control sample.

Table 4: Dilepton control samples that are combined when estimating the lost-lepton background.

Label	Selection			p_T^{miss} bins [GeV]
A0	2–3 jets,	$t_{\text{mod}} > 10$,	$M_{\ell b} \leq 175$ GeV	[600, 750, $+\infty$]
B	2–3 jets,	$t_{\text{mod}} > 10$,	$M_{\ell b} > 175$ GeV	[450, 700, $+\infty$]
C	≥ 4 jets,	$t_{\text{mod}} \leq 0$,	$M_{\ell b} \leq 175$ GeV	[650, 800, $+\infty$]
E0	≥ 4 jets,	$0 < t_{\text{mod}} \leq 10$,	$M_{\ell b} \leq 175$ GeV	[450, 600, $+\infty$]
G0	≥ 4 jets,	$t_{\text{mod}} > 10$,	$M_{\ell b} \leq 175$ GeV	[550, 750, $+\infty$]
H	≥ 4 jets,	$t_{\text{mod}} > 10$,	$M_{\ell b} > 175$ GeV	[250, 500, $+\infty$]
I	≥ 5 jets,	$N_{b, \text{med}} \geq 1$,	$N_{b, \text{soft}} \geq 0$	[550, 750, $+\infty$]
J	≥ 3 jets,	$N_{b, \text{med}} \geq 0$,	$N_{b, \text{soft}} \geq 1$	[550, 750, $+\infty$]

in the b tagging efficiency and in the choices of the renormalization and factorization scales are small. The total uncertainty in the transfer factor is 6–100%, depending on the region. The uncertainty in the transfer factor is typically comparable to the statistical uncertainty in the control sample yield. Associated uncertainties in the $k(p_T^{\text{miss}})$ extrapolation factor used in the regions shown in Table 4 were derived from an orthogonal $t\bar{t}$ enriched dilepton sample. The leading uncertainty associated with the p_T^{miss} extrapolation is the statistical uncertainty in the simulated samples (5–60%).

5.2 One-lepton background

The one-lepton (1ℓ) background is suppressed by the $p_T^{\text{miss}} > 250$ GeV and $M_T > 150$ GeV requirements. This suppression is more effective for events with a W boson originating from a top quark decay than for direct W boson production ($W + \text{jets}$). In the case of a top quark

decay, the mass of the top quark sets bound at the mass of the lepton-neutrino system. As a result, the contribution of semileptonic $t\bar{t}$ events to the tail of the M_T distribution is caused by p_T^{miss} resolution effects, while in the case of $W + \text{jets}$ events the contribution from off-shell W bosons is dominant.

The semileptonic $t\bar{t}$ background is taken from simulation. Studies with simulated samples indicate that the contribution to the total background from semileptonic $t\bar{t}$ events is less than 10% in most search regions, except in a few regions with ≥ 1 top quark tags, where the contribution becomes as large as 30% [29]. An uncertainty of 100% is assigned to cover the impact of the uncertainties in the p_T^{miss} resolution as measured in a photon data sample.

The $W + \text{jets}$ background is estimated from a control sample with no b-tagged jets nor soft b objects (0b sample) obtained by inverting the b-tagging requirement. Figure 4 (right) shows the $M_{\ell b}$ distribution in the 0b control sample, where this quantity is computed from the jet with the highest value of the DeepCSV discriminant. The modeling of this distribution in simulation is validated by comparing simulation and data in a $W + \text{jets}$ enriched control sample obtained by selecting events with 1–2 jets and $60 < M_T < 120 \text{ GeV}$.

The $W + \text{jets}$ background estimate in each search region is obtained from the yield in the corresponding control samples and a transfer factor determined from simulation. These control samples are shown to have high purity (70–80%) of the $W + \text{jets}$ process in places where this background is more significant in the corresponding ($M_{\ell b} > 175 \text{ GeV}$) search region. In other cases, the purity can go down to 50%. Contamination from lost-lepton and other processes are subtracted from the control sample data yields. The transfer factor, defined as the ratio of the expected one lepton (not from t) yield in the signal region and the yield of events in the 0b control sample, accounts for the acceptance and the b tagging efficiency. The transfer factors are validated by checking the differences in performance of the b tagging algorithm and the off-shell W production modeling between data and simulation. Corrections are applied for differences in b tagging efficiencies between data and simulation. The $W + \text{jets}$ kinematic properties in the 0b control sample show good agreement between data and simulation as shown in Figure 4. As in the case of the lost-lepton background estimate, multiple control samples are combined into a single control sample until the expected yield in simulation is at least five events, as detailed in Table 5.

The dominant uncertainties in the transfer factors are the statistical uncertainties in the simulated samples, the uncertainties in the b tagging efficiencies, and the $W + b(\bar{b})$ cross section.

Table 5: Search regions where the corresponding 0b control samples are combined when estimating the $W + \text{jets}$ background.

Label	Selection			p_T^{miss} bins [GeV]
C	≥ 4 jets,	$t_{\text{mod}} \leq 0,$	$M_{\ell b} \leq 175 \text{ GeV}$	[650, 800, $+\infty$]
E0	≥ 4 jets,	$0 < t_{\text{mod}} \leq 10,$	$M_{\ell b} \leq 175 \text{ GeV}$	[450, 600, $+\infty$]
G0	≥ 4 jets,	$t_{\text{mod}} > 10,$	$M_{\ell b} \leq 175 \text{ GeV}$	[550, 750, $+\infty$]

5.3 Background from events containing $Z \rightarrow \nu\bar{\nu}$

The third category arises from $t\bar{t}Z$, WZ , and other rare multiboson processes. In all these processes, events from a leptonically decaying W boson, and one or more Z bosons decaying to neutrinos, enter the search regions. In most search regions, $t\bar{t}Z$ is the most important process contributing to this category. These backgrounds are estimated from simulation. The contribution from $t\bar{t}Z$ is normalized using the measured value of the cross section [91]. This normalization results in a rescaling of the theoretical cross section by $1.17^{+0.10}_{-0.09}$, where the uncertainty is

taken from the statistical uncertainty in the measurement.

6 Systematic uncertainties

The contributions to the total uncertainty in the estimated backgrounds and expected signal yields are summarized in Table 6. The total uncertainty is generally larger at higher p_T^{miss} or when yields in the control samples become small. Out of the uncertainties quoted, the theoretical uncertainties are correlated across the different data-taking periods because they are independent of the data-taking period. The uncertainties on lepton efficiency are also assumed to be fully correlated, but other experimental uncertainties are taken as uncorrelated between the different data-taking years.

Table 6: Summary of major systematic uncertainties. The range of values reflect their impact on the estimated backgrounds and signal yields in different signal regions. A 100% uncertainty is assigned to the 1ℓ (from t) background estimated from simulation.

Source	Signal	Lost lepton	1ℓ (not from t)	$Z \rightarrow \nu\bar{\nu}$
Data statistical uncertainty	—	5–50%	4–30%	—
Simulation statistical uncertainty	6–36%	3–68%	5–70%	4–41%
$t\bar{t}$ p_T^{miss} modeling	—	3–50%	—	—
Signal p_T^{miss} modeling	1–25%	—	—	—
QCD scales	1–5%	0–3%	2–5%	1–40%
Parton distribution	—	0–4%	1–8%	1–12%
Pileup	1–5%	1–8%	0–5%	0–7%
Luminosity	2.3–2.5%	—	—	2.3–2.5%
$W + b(\bar{b})$ cross section	—	—	20–40%	—
$t\bar{t}Z$ cross section	—	—	—	5–10%
System recoil (ISR)	1–13%	0–3%	—	—
Jet energy scale	2–24%	1–16%	1–34%	1–28%
p_T^{miss} resolution	—	1–10%	1–5%	—
Trigger	2–3%	1–3%	—	2–3%
Lepton efficiency	3–4%	2–12%	—	1–2%
Merged t tagging efficiency	3–6%	—	—	5–10%
Resolved t tagging efficiency	5–6%	—	—	3–5%
b tagging efficiency	0–2%	0–1%	1–7%	1–10%
Soft b tagging efficiency	2–3%	0–1%	0–1%	0–5%

Theoretical uncertainties affect all quantities derived from simulation such as the signal acceptance, the transfer factors used in the estimate of the lost lepton and one-lepton backgrounds, and the estimate of the $Z \rightarrow \nu\bar{\nu}$ background. The uncertainty resulting from missing higher-order corrections is estimated by varying the renormalization and factorization scales by a factor of two [92, 93] with the two scales taken to be the same in each variation. The effect of the uncertainties in the parton distribution functions is estimated using 100 variations provided with the NNPDF sets, and the effect of the uncertainty in the value of the strong coupling constant is estimated by varying the value $\alpha_s(m_Z) = 0.1180$ by ± 0.0015 [94]. All theory uncertainties are varied based on the NNPDF3.0 scheme.

The p_T^{miss} lineshape is corrected to account for mismodeling effects from p_T^{miss} resolution and $N_j^{\text{ISR/FSR}}$. The uncertainty in these corrections results in a 1–50% uncertainty in the estimated backgrounds, depending on signal region. The uncertainty in the $N_j^{\text{ISR/FSR}}$ rescaling also affects

the signal acceptance. The effect is small in most search regions, but can be noticeable in signal scenarios with a compressed mass spectrum.

The effect of the uncertainty in the jet energy scale is 1–34% in the estimated backgrounds and up to 24% in the signal acceptance. Variations in the efficiency of the b jet and soft b object identification typically affect the estimated signal and background yields by 0.1% and 3%, with a full range up to 10%.

The uncertainty in the cross section of $W + \text{jets}$ events with jets containing b quarks is an important source of uncertainty in the estimation of the $W + \text{jets}$ background. A comparison of the multiplicity of b-tagged jets between data and simulation is performed in a $W + \text{jets}$ enriched control sample obtained with the same selection as for the $M_{\ell b}$ validation test, with the additional requirement of $p_T^{\text{miss}} > 250 \text{ GeV}$. From this study, we estimate a 50% uncertainty in the $W + b(\bar{b})$ cross section resulting in a 20–40% uncertainty in the $W + \text{jets}$ background estimate.

7 Results and interpretation

The event yields and the SM predictions in the search regions are summarized in Tables 7 and 8. These results are also illustrated in Fig. 5. The observed yields are consistent with the estimated SM backgrounds. Isolated fluctuations are observed in a few signal region bins. The data events in these signal region bins were inspected carefully to determine if any detector or reconstruction effects were the source of the high p_T^{miss} . No such issues were detected.

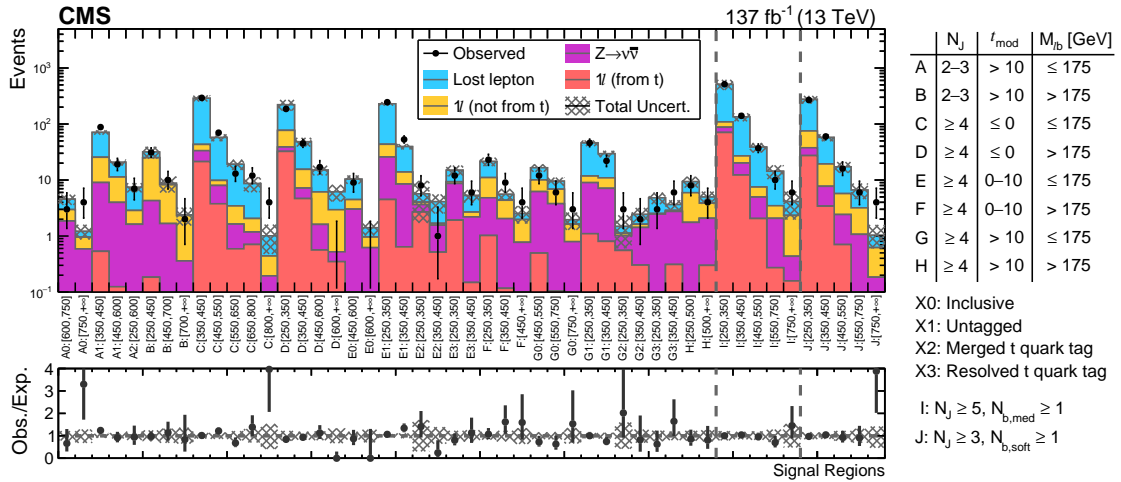


Figure 5: The observed and expected yields in Tables 7 and 8 and their ratios are shown as stacked histograms. The lost lepton and 1ℓ (not from t) are estimated from data-driven methods, while 1ℓ (from t) and $Z \rightarrow \nu\bar{\nu}$ backgrounds are taken from simulation. The uncertainties consist of statistical and systematic components summed in quadrature and are shown as shaded bands.

Results are interpreted in the context of top squark pair production models described in Section 1. For a given model, 95% confidence level (CL) upper limits on the production cross sections are derived as a function of the mass of the SUSY particles. The search regions are combined using a modified frequentist approach, employing the CL_s criterion and an asymptotic formulation [95–98]. The likelihood function is constructed by multiplying the probability density functions from each search region. These probability density functions are products of Poisson functions for the control region yields and log-normal constraint functions for the

Table 7: The observed and expected yields in the standard search regions. For the top quark tagging categories, we use the abbreviations U for untagged, M for merged, and R for resolved.

Label	N_j	t_{mod}	$M_{t\bar{b}}$ [GeV]	t cat.	p_T^{miss} [GeV]	Lost lepton	1 ℓ (not from t)	1 ℓ (from t)	$Z \rightarrow \nu\bar{\nu}$	Total expected	Total observed
A0				—	600–750	1.6 ± 0.7	1.1 ± 0.5	0.09 ± 0.09	1.8 ± 0.4	4.5 ± 0.9	3
					750– $+\infty$	0.26 ± 0.19	0.37 ± 0.28	—	0.59 ± 0.20	1.2 ± 0.4	4
A1	2–3	>10	≤ 175	U	350–450	46 ± 5	16 ± 5	0.5 ± 0.5	8.5 ± 1.2	71 ± 8	88
					450–600	9.4 ± 1.5	7.3 ± 2.4	0.12 ± 0.12	3.9 ± 0.7	20.7 ± 3.0	19
A2				M	250–600	4.5 ± 1.1	1.2 ± 0.4	0.03 ± 0.03	1.6 ± 0.4	7.4 ± 1.3	7
					250–450	6.6 ± 1.5	21 ± 10	0.18 ± 0.18	4.1 ± 0.9	32 ± 11	31
B	2–3	>10	>175	—	450–700	0.55 ± 0.26	7 ± 4	—	1.7 ± 0.5	9 ± 4	10
					700– $+\infty$	0.07 ± 0.06	2.0 ± 1.1	—	0.36 ± 0.15	2.4 ± 1.1	2
C	≥ 4	≤ 0	≤ 175	—	350–450	245 ± 23	9.8 ± 3.5	21 ± 21	12.1 ± 2.7	289 ± 32	293
					450–550	48 ± 7	1.8 ± 0.7	4 ± 4	4.2 ± 0.9	58 ± 8	70
					550–650	16 ± 4	1.8 ± 1.0	0.6 ± 0.6	1.04 ± 0.31	19 ± 4	13
					650–800	6.6 ± 2.5	0.9 ± 0.4	0.7 ± 0.7	0.47 ± 0.19	8.6 ± 2.6	12
D	≥ 4	≤ 0	>175	—	800– $+\infty$	0.6 ± 0.7	0.25 ± 0.13	0.08 ± 0.08	0.12 ± 0.08	1.0 ± 0.7	4
					250–350	144 ± 13	38 ± 13	32 ± 32	6.5 ± 1.5	221 ± 37	186
					350–450	33 ± 5	8.3 ± 3.4	5 ± 5	2.5 ± 0.7	48 ± 8	45
					450–600	8.9 ± 2.5	4.5 ± 1.9	0.6 ± 0.6	1.05 ± 0.26	15.0 ± 3.2	17
E0				—	600– $+\infty$	3.2 ± 2.1	2.4 ± 0.9	0.35 ± 0.35	0.17 ± 0.16	6.2 ± 2.4	0
					450–600	5.9 ± 1.5	1.4 ± 0.7	—	3.0 ± 0.7	10.4 ± 1.8	9
E1	≥ 4	0–10	≤ 175	U	600– $+\infty$	0.45 ± 0.28	0.34 ± 0.18	—	0.62 ± 0.24	1.4 ± 0.4	0
					250–350	186 ± 17	18 ± 6	4 ± 4	21 ± 4	230 ± 19	245
E2				M	350–450	26 ± 4	5.4 ± 1.8	0.6 ± 0.6	7.8 ± 1.3	40 ± 4	53
					250–350	1.7 ± 0.9	0.38 ± 0.16	2.7 ± 2.7	0.95 ± 0.27	5.7 ± 2.8	8
E3				R	350–450	2.4 ± 1.4	0.12 ± 0.12	0.5 ± 0.5	1.05 ± 0.29	4.1 ± 1.5	1
					250–350	5.6 ± 1.8	0.7 ± 0.4	1.9 ± 1.9	6.8 ± 1.5	15.0 ± 3.0	12
F	≥ 4	0–10	>175	—	350–450	2.6 ± 1.4	0.48 ± 0.25	0.15 ± 0.15	2.0 ± 0.5	5.3 ± 1.5	6
					250–350	10.4 ± 2.5	6.2 ± 3.2	1.0 ± 1.0	3.8 ± 0.8	21 ± 4	23
					450– $+\infty$	$0.5^{+1.0}_{-0.5}$	1.2 ± 0.7	0.08 ± 0.08	0.69 ± 0.25	2.5 ± 1.2	4
G0				—	450–550	6.5 ± 1.9	3.8 ± 1.7	0.5 ± 0.5	5.7 ± 1.0	16.6 ± 2.8	12
					550–750	2.7 ± 1.2	3.1 ± 1.2	0.1 ± 0.1	3.7 ± 0.8	9.5 ± 1.9	6
					750– $+\infty$	0.33 ± 0.18	0.83 ± 0.35	—	0.79 ± 0.16	1.9 ± 0.4	3
G1	≥ 4	>10	≤ 175	U	250–350	34 ± 5	2.8 ± 1.2	1.1 ± 1.1	7.9 ± 1.8	46 ± 6	46
					350–450	19 ± 4	3.8 ± 1.6	0.8 ± 0.8	6.3 ± 1.5	30 ± 4	22
G2				M	250–350	0.37 ± 0.27	0.1 ± 0.06	0.6 ± 0.6	0.46 ± 0.15	1.5 ± 0.6	3
					350–450	0.8 ± 0.5	0.2 ± 0.1	0.3 ± 0.3	1.12 ± 0.23	2.4 ± 0.6	2
G3				R	250–350	2.3 ± 1.0	0.06 ± 0.09	0.09 ± 0.09	2.4 ± 0.5	4.8 ± 1.2	3
					350–450	0.8 ± 0.5	0.12 ± 0.08	0.31 ± 0.31	2.4 ± 0.6	3.6 ± 0.8	6
H	≥ 4	>10	>175	—	250–500	3.4 ± 1.4	4.2 ± 2.0	0.09 ± 0.09	1.7 ± 0.4	9.4 ± 2.5	8
					500– $+\infty$	1.1 ± 0.5	1.8 ± 1.0	0.3 ± 0.3	1.8 ± 0.6	5.0 ± 1.3	4

nuisance parameters, with correlated parameters among the search regions being accounted for. When computing the limit, the expected signal yields are corrected for the possible contributions of signal events to the control samples. These corrections are typically around 5–10%.

For the models in which both top squarks decay to a top quark and an $\tilde{\chi}_1^0$, the limits are derived from the $\Delta m(\tilde{t}, \tilde{\chi}_1^0) \sim m_W$ search regions when $100 \leq \Delta m(\tilde{t}, \tilde{\chi}_1^0) \leq 150$ GeV, and from the $\Delta m(\tilde{t}, \tilde{\chi}_1^0) \sim m_t$ search regions when $150 \leq \Delta m(\tilde{t}, \tilde{\chi}_1^0) \leq 225$ GeV. For all other models, the cross section limits are obtained from the standard search regions.

In the case of $\Delta m(\tilde{t}, \tilde{\chi}_1^0) \sim m_W$, the specially designed signal regions result in improvements of up to a factor of five in cross section sensitivity with respect to the results that would have been obtained based on the standard search regions. On the other hand, the corresponding improvements from the signal regions designed for $\Delta m(\tilde{t}, \tilde{\chi}_1^0) \sim m_t$ are typically of the order of 10–20%. In the high mass region, this analysis is sensitive to an additional ~ 200 GeV in

Table 8: The observed and expected yields for signal regions targeting scenarios of top squark production with a compressed mass spectrum.

Label	N_j	$N_{b, \text{med}}$	$N_{b, \text{soft}}$	p_T^{miss} [GeV]	Lost lepton	1ℓ (not from t)	1ℓ (from t)	$Z \rightarrow \nu\bar{\nu}$	Total expected	Total observed
I	≥ 5	≥ 1	≥ 0	250–350	403 ± 40	21 ± 8	71 ± 71	17 ± 4	511 ± 81	513
				350–450	108 ± 15	6.8 ± 2.5	12 ± 12	7.8 ± 1.6	134 ± 19	140
				450–550	31 ± 8	2.5 ± 1.0	2.0 ± 2.0	2.9 ± 0.8	39 ± 8	37
				550–750	11 ± 5	1.4 ± 0.6	0.27 ± 0.27	1.8 ± 0.5	14 ± 5	10
				750– $+\infty$	1.8 ± 1.1	$1.9^{+2.5}_{-1.9}$	0.16 ± 0.16	0.28 ± 0.10	4.1 ± 2.5	6
J	≥ 3	≥ 0	≥ 1	250–350	201 ± 21	37 ± 7	27 ± 27	10.4 ± 1.5	276 ± 35	268
				350–450	38 ± 7	11.6 ± 2.2	3.4 ± 3.4	4.3 ± 0.9	58 ± 8	60
				450–550	11.5 ± 3.5	3.3 ± 0.6	0.7 ± 0.7	1.7 ± 0.6	17 ± 4	16
				550–750	3.5 ± 2.3	2.1 ± 0.5	—	1.1 ± 0.8	6.6 ± 2.5	6
				750– $+\infty$	0.4 ± 0.4	0.44 ± 0.16	0.02 ± 0.02	0.2 ± 0.4	1.0 ± 0.6	4

expected limit for top squark masses [29].

The 95% CL upper limits on cross sections for the $pp \rightarrow \tilde{t}\tilde{t} \rightarrow \tilde{t}\tilde{t}\tilde{\chi}_1^0\tilde{\chi}_1^0$ process, as a function of sparticle masses and assuming that the top quarks are not polarized, are shown in Fig. 6. In this figure we also show the excluded region of parameter space based on the expected cross section for top squark pair production. We exclude the existence of top squarks with masses up to 1.2 TeV for a massless neutralino, and neutralinos with masses up to 600 GeV for $m_{\tilde{t}} = 1$ TeV. The most sensitive search regions for these processes are those with high t_{mod} and low $M_{\ell b}$ values. Signal models with higher $\Delta m(\tilde{t}, \tilde{\chi}_1^0)$ are more sensitive in the regions with higher p_T^{miss} . The white band corresponds to the region $|m_{\tilde{t}} - m_{\tilde{t}} - m_{\tilde{\chi}_1^0}| < 25$ GeV, $m_{\tilde{t}} < 275$ GeV, where the selection acceptance for top squark pair production changes rapidly. In this region the acceptance is very sensitive to the details of the simulation, and therefore no interpretation is performed.

Figures 7 and 8 display the equivalent limits for the $pp \rightarrow \tilde{t}\tilde{t} \rightarrow \tilde{b}\tilde{b}\tilde{\chi}_1^\pm\tilde{\chi}_1^\pm$ ($\tilde{\chi}_1^\pm \rightarrow W\tilde{\chi}_1^0$) and $pp \rightarrow \tilde{t}\tilde{t} \rightarrow \tilde{t}\tilde{b}\tilde{\chi}_1^\pm\tilde{\chi}_1^0$ ($\tilde{\chi}_1^\pm \rightarrow W^*\tilde{\chi}_1^0$) scenarios, respectively. The search regions with high $M_{\ell b}$ are most sensitive to these models. These models are characterized by three mass parameters (for the top squark, the chargino, and the neutralino). In the mixed decay scenario of Fig. 8, we have assumed a compressed mass spectrum for the neutralino-chargino pair, which is theoretically favored if the $\tilde{\chi}_1^\pm$ and the $\tilde{\chi}_1^0$ are higgsinos. The search has very poor sensitivity for models with this mass spectrum when both top squarks decay to charginos. Therefore in the case of Fig. 7, we have chosen a larger $\tilde{\chi}_1^\pm$ mass splitting between the $\tilde{\chi}_1^\pm$ and the $\tilde{\chi}_1^0$.

8 Summary

A search for direct top squark pair production is performed using events with one lepton, jets, and significant missing transverse momentum. The search is based on proton-proton collision data at a center-of-mass energy of 13 TeV recorded by the CMS experiment at the LHC during 2016–2018 and corresponding to an integrated luminosity of 137 fb^{-1} . The leading backgrounds in this analysis, mainly dileptonic $\tilde{t}\tilde{t}$ decays, where one of the leptons is not reconstructed or identified, and $W + \text{jets}$ production are estimated from data control regions. The semileptonic $\tilde{t}\tilde{t}$ and $Z \rightarrow \nu\bar{\nu}$ backgrounds are taken from simulation. No significant deviations from the standard model expectations are observed. Limits on pair-produced top squarks are established in the context of supersymmetry models conserving R -parity. Exclusion limits at 95% CL for top squark masses up to 1.2 TeV are set for a massless neutralino. For models with a top squark mass of 1 TeV, neutralino masses up to 600 GeV are excluded.

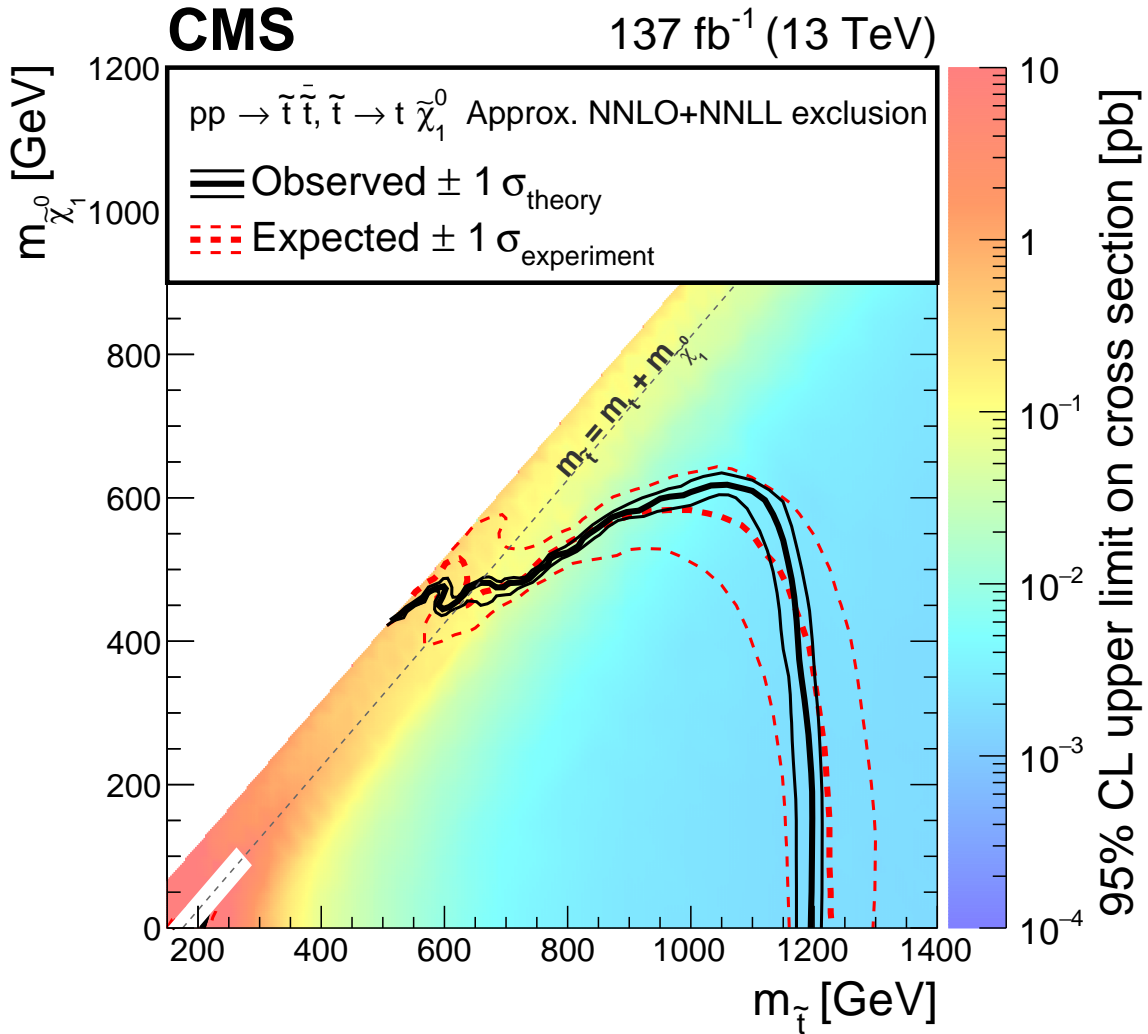


Figure 6: Exclusion limits at 95% CL for the $pp \rightarrow \tilde{t}\tilde{t}^* \rightarrow t\tilde{t}\tilde{\chi}_1^0\tilde{\chi}_1^0$ scenario. The colored map illustrates the 95% CL upper limits on the product of the production cross section and branching fraction. The area enclosed by the thick black curve represents the observed exclusion region, and that enclosed by the thick, dashed red curve represents the expected exclusion. The thin dotted (red) curves indicate the region containing 68% of the distribution of limits expected under the background-only hypothesis. The thin solid (black) curves show the change in the observed limit by varying the signal cross sections within their theoretical uncertainties. The white band excluded from the limits corresponds to the region $|m_{\tilde{t}} - m_t - m_{\tilde{\chi}_1^0}| < 25 \text{ GeV}$, $m_{\tilde{t}} < 275 \text{ GeV}$, where the selection acceptance for top squark pair production changes rapidly and is therefore very sensitive to the details of the simulation.

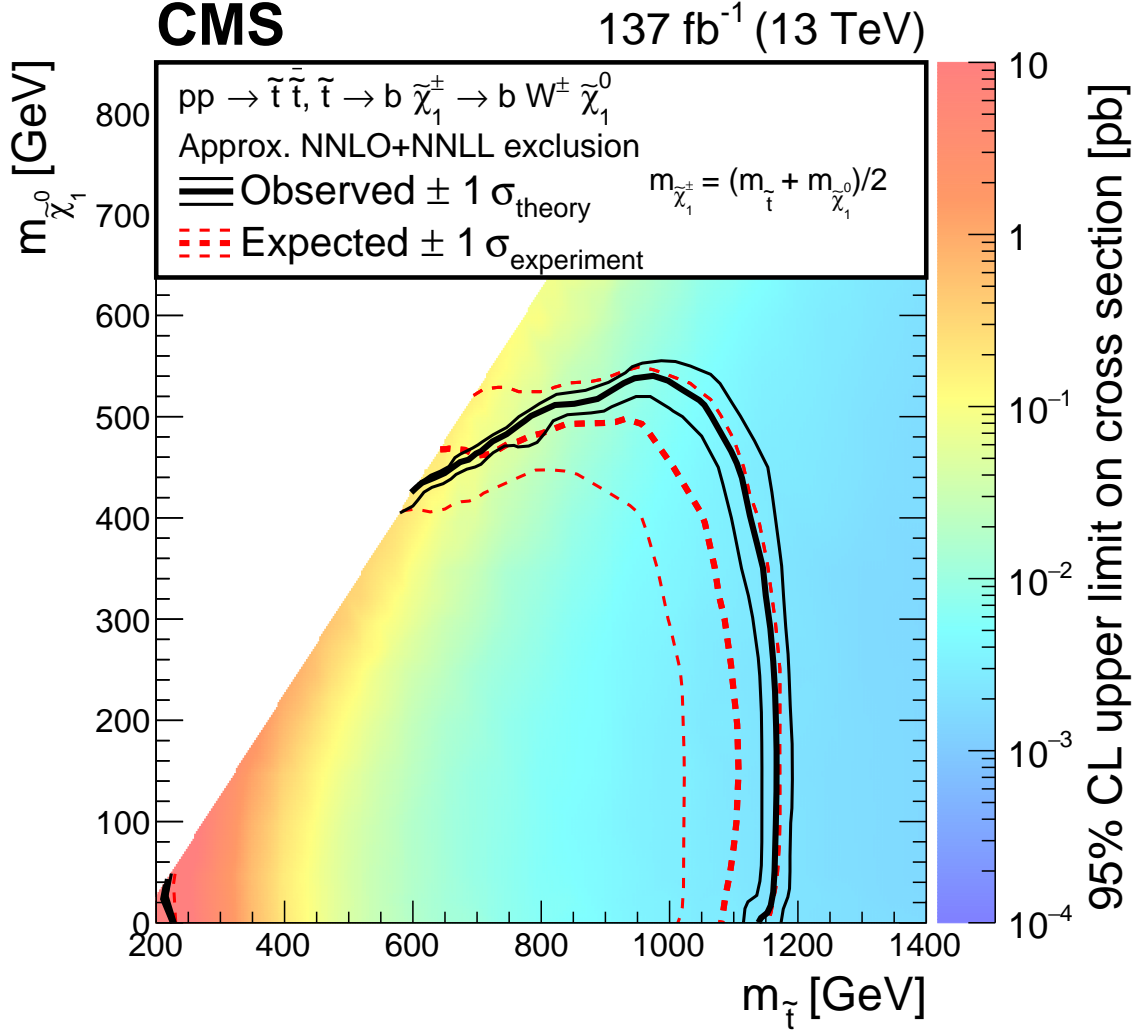


Figure 7: Exclusion limits at 95% CL for the $pp \rightarrow \tilde{t}\tilde{t}^* \rightarrow b\bar{b}\tilde{\chi}_1^\pm\tilde{\chi}_1^\pm$ ($\tilde{\chi}_1^\pm \rightarrow W\tilde{\chi}_1^0$) scenario. The mass of $\tilde{\chi}_1^\pm$ is chosen to be $(m_{\tilde{t}} + m_{\tilde{\chi}_1^0})/2$. The colored map illustrates the 95% CL upper limits on the product of the production cross section and branching fraction. The area enclosed by the thick black curve represents the observed exclusion region, and that enclosed by the thick, dashed red curve represents the expected exclusion. The thin dotted (red) curves indicate the region containing 68% of the distribution of limits expected under the background-only hypothesis. The thin solid (black) curves show the change in the observed limit by varying the signal cross sections within their theoretical uncertainties.

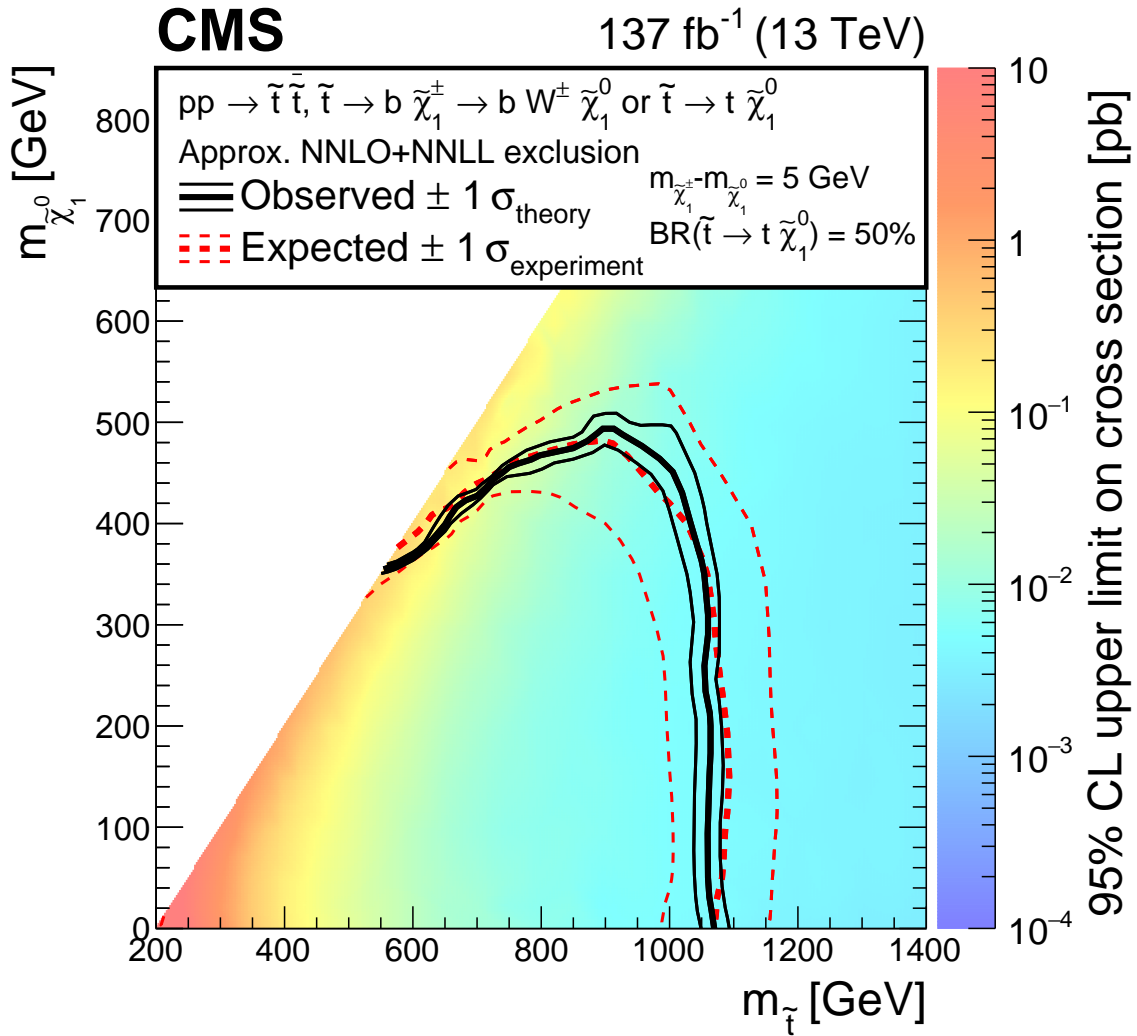


Figure 8: Exclusion limits at 95% CL for the $pp \rightarrow \tilde{t}\tilde{t}^* \rightarrow t\tilde{t} \tilde{\chi}_1^\pm \tilde{\chi}_1^0$ ($\tilde{\chi}_1^\pm \rightarrow W^* \tilde{\chi}_1^0$) scenario. The mass difference between the $\tilde{\chi}_1^\pm$ and the $\tilde{\chi}_1^0$ is taken to be 5 GeV. The colored map illustrates the 95% CL upper limits on the product of the production cross section and branching fraction. The area enclosed by the thick black curve represents the observed exclusion region, and that enclosed by the thick, dashed red curve represents the expected exclusion. The thin dotted (red) curves indicate the region containing 68% of the distribution of limits expected under the background-only hypothesis. The thin solid (black) curves show the change in the observed limit by varying the signal cross sections within their theoretical uncertainties.

Acknowledgments

We congratulate our colleagues in the CERN accelerator departments for the excellent performance of the LHC and thank the technical and administrative staffs at CERN and at other CMS institutes for their contributions to the success of the CMS effort. In addition, we gratefully acknowledge the computing centers and personnel of the Worldwide LHC Computing Grid for delivering so effectively the computing infrastructure essential to our analyses. Finally, we acknowledge the enduring support for the construction and operation of the LHC and the CMS detector provided by the following funding agencies: BMBWF and FWF (Austria); FNRS and FWO (Belgium); CNPq, CAPES, FAPERJ, FAPERGS, and FAPESP (Brazil); MES (Bulgaria); CERN; CAS, MoST, and NSFC (China); COLCIENCIAS (Colombia); MSES and CSF (Croatia); RPF (Cyprus); SENESCYT (Ecuador); MoER, ERC IUT, PUT and ERDF (Estonia); Academy of Finland, MEC, and HIP (Finland); CEA and CNRS/IN2P3 (France); BMBF, DFG, and HGF (Germany); GSRT (Greece); NKFI (Hungary); DAE and DST (India); IPM (Iran); SFI (Ireland); INFN (Italy); MSIP and NRF (Republic of Korea); MES (Latvia); LAS (Lithuania); MOE and UM (Malaysia); BUAP, CINVESTAV, CONACYT, LNS, SEP, and UASLP-FAI (Mexico); MOS (Montenegro); MBIE (New Zealand); PAEC (Pakistan); MSHE and NSC (Poland); FCT (Portugal); JINR (Dubna); MON, RosAtom, RAS, RFBR, and NRC KI (Russia); MESTD (Serbia); SEIDI, CPAN, PCTI, and FEDER (Spain); MOSTR (Sri Lanka); Swiss Funding Agencies (Switzerland); MST (Taipei); ThEPCenter, IPST, STAR, and NSTDA (Thailand); TUBITAK and TAEK (Turkey); NASU (Ukraine); STFC (United Kingdom); DOE and NSF (USA).

Individuals have received support from the Marie-Curie program and the European Research Council and Horizon 2020 Grant, contract Nos. 675440, 752730, and 765710 (European Union); the Leventis Foundation; the A.P. Sloan Foundation; the Alexander von Humboldt Foundation; the Belgian Federal Science Policy Office; the Fonds pour la Formation à la Recherche dans l'Industrie et dans l'Agriculture (FRIA-Belgium); the Agentschap voor Innovatie door Wetenschap en Technologie (IWT-Belgium); the F.R.S.-FNRS and FWO (Belgium) under the "Excellence of Science – EOS" – be.h project n. 30820817; the Beijing Municipal Science & Technology Commission, No. Z181100004218003; the Ministry of Education, Youth and Sports (MEYS) of the Czech Republic; the Lendület ("Momentum") Program and the János Bolyai Research Scholarship of the Hungarian Academy of Sciences, the New National Excellence Program ÚNKP, the NKFI research grants 123842, 123959, 124845, 124850, 125105, 128713, 128786, and 129058 (Hungary); the Council of Science and Industrial Research, India; the HOMING PLUS program of the Foundation for Polish Science, cofinanced from European Union, Regional Development Fund, the Mobility Plus program of the Ministry of Science and Higher Education, the National Science Center (Poland), contracts Harmonia 2014/14/M/ST2/00428, Opus 2014/13/B/ST2/02543, 2014/15/B/ST2/03998, and 2015/19/B/ST2/02861, Sonata-bis 2012/07/E/ST2/01406; the National Priorities Research Program by Qatar National Research Fund; the Ministry of Science and Education, grant no. 3.2989.2017 (Russia); the Programa Estatal de Fomento de la Investigación Científica y Técnica de Excelencia María de Maeztu, grant MDM-2015-0509 and the Programa Severo Ochoa del Principado de Asturias; the Thalís and Aristeia programs cofinanced by EU-ESF and the Greek NSRF; the Rachadapisek Sompot Fund for Postdoctoral Fellowship, Chulalongkorn University and the Chulalongkorn Academic into Its 2nd Century Project Advancement Project (Thailand); the Welch Foundation, contract C-1845; and the Weston Havens Foundation (USA).

References

- [1] P. Ramond, "Dual theory for free fermions", *Phys. Rev. D* **3** (1971) 2415, doi:10.1103/PhysRevD.3.2415.
- [2] Y. A. Gol'fand and E. P. Likhtman, "Extension of the algebra of Poincare group generators and violation of P invariance", *JETP Lett.* **13** (1971) 323. [Pisma Zh. Eksp. Teor. Fiz. 13 (1971) 452].
- [3] A. Neveu and J. H. Schwarz, "Factorizable dual model of pions", *Nucl. Phys. B* **31** (1971) 86, doi:10.1016/0550-3213(71)90448-2.
- [4] D. V. Volkov and V. P. Akulov, "Possible universal neutrino interaction", *JETP Lett.* **16** (1972) 438. [Pisma Zh. Eksp. Teor. Fiz. 16 (1972) 621].
- [5] J. Wess and B. Zumino, "A Lagrangian model invariant under supergauge transformations", *Phys. Lett. B* **49** (1974) 52, doi:10.1016/0370-2693(74)90578-4.
- [6] J. Wess and B. Zumino, "Supergauge transformations in four-dimensions", *Nucl. Phys. B* **70** (1974) 39, doi:10.1016/0550-3213(74)90355-1.
- [7] P. Fayet, "Supergauge invariant extension of the Higgs mechanism and a model for the electron and its neutrino", *Nucl. Phys. B* **90** (1975) 104, doi:10.1016/0550-3213(75)90636-7.
- [8] H. P. Nilles, "Supersymmetry, supergravity and particle physics", *Phys. Rept.* **110** (1984) 1, doi:10.1016/0370-1573(84)90008-5.
- [9] G. R. Farrar and P. Fayet, "Phenomenology of the production, decay, and detection of new hadronic states associated with supersymmetry", *Phys. Lett. B* **76** (1978) 575, doi:10.1016/0370-2693(78)90858-4.
- [10] G. Jungman, M. Kamionkowski, and K. Griest, "Supersymmetric dark matter", *Phys. Rept.* **267** (1996) 195, doi:10.1016/0370-1573(95)00058-5, arXiv:hep-ph/9506380.
- [11] G. 't Hooft, "Naturalness, chiral symmetry, and spontaneous chiral symmetry breaking", *NATO Sci. Ser. B* **59** (1980) 135, doi:10.1007/978-1-4684-7571-5_9.
- [12] M. Dine, W. Fischler, and M. Srednicki, "Supersymmetric technicolor", *Nucl. Phys. B* **189** (1981) 575, doi:10.1016/0550-3213(81)90582-4.
- [13] S. Dimopoulos and S. Raby, "Supercolor", *Nucl. Phys. B* **192** (1981) 353, doi:10.1016/0550-3213(81)90430-2.
- [14] S. Dimopoulos and H. Georgi, "Softly broken supersymmetry and SU(5)", *Nucl. Phys. B* **193** (1981) 150, doi:10.1016/0550-3213(81)90522-8.
- [15] R. K. Kaul and P. Majumdar, "Cancellation of quadratically divergent mass corrections in globally supersymmetric spontaneously broken gauge theories", *Nucl. Phys. B* **199** (1982) 36, doi:10.1016/0550-3213(82)90565-X.
- [16] ATLAS Collaboration, "Search for top squarks in final states with one isolated lepton, jets, and missing transverse momentum in $\sqrt{s} = 13$ TeV pp collisions with the ATLAS detector", *Phys. Rev. D* **94** (2016) 052009, doi:10.1103/PhysRevD.94.052009, arXiv:1606.03903.

-
- [17] ATLAS Collaboration, “Search for heavy long-lived charged R-hadrons with the ATLAS detector in 3.2 fb^{-1} of proton–proton collision data at $\sqrt{s} = 13 \text{ TeV}$ ”, *Phys. Lett. B* **760** (2016) 647, doi:10.1016/j.physletb.2016.07.042, arXiv:1606.05129.
- [18] ATLAS Collaboration, “Search for direct top squark pair production in events with a Higgs or Z boson, and missing transverse momentum in $\sqrt{s} = 13 \text{ TeV}$ pp collisions with the ATLAS detector”, *JHEP* **08** (2017) 006, doi:10.1007/JHEP08(2017)006, arXiv:1706.03986.
- [19] ATLAS Collaboration, “Search for direct top squark pair production in final states with two leptons in $\sqrt{s} = 13 \text{ TeV}$ pp collisions with the ATLAS detector”, *Eur. Phys. J. C* **77** (2017) 898, doi:10.1140/epjc/s10052-017-5445-x, arXiv:1708.03247.
- [20] ATLAS Collaboration, “Search for a scalar partner of the top quark in the jets plus missing transverse momentum final state at $\sqrt{s} = 13 \text{ TeV}$ with the ATLAS detector”, *JHEP* **12** (2017) 085, doi:10.1007/JHEP12(2017)085, arXiv:1709.04183.
- [21] ATLAS Collaboration, “Search for $B - L$ R-parity-violating top squarks in $\sqrt{s} = 13 \text{ TeV}$ pp collisions with the ATLAS experiment”, *Phys. Rev. D* **97** (2018) 032003, doi:10.1103/PhysRevD.97.032003, arXiv:1710.05544.
- [22] ATLAS Collaboration, “A search for pair-produced resonances in four-jet final states at $\sqrt{s} = 13 \text{ TeV}$ with the ATLAS detector”, *Eur. Phys. J. C* **78** (2018) 250, doi:10.1140/epjc/s10052-018-5693-4, arXiv:1710.07171.
- [23] ATLAS Collaboration, “Search for top-squark pair production in final states with one lepton, jets, and missing transverse momentum using 36 fb^{-1} of $\sqrt{s} = 13 \text{ TeV}$ pp collision data with the ATLAS detector”, *JHEP* **06** (2018) 108, doi:10.1007/JHEP06(2018)108, arXiv:1711.11520.
- [24] ATLAS Collaboration, “Search for top squarks decaying to tau sleptons in pp collisions at $\sqrt{s} = 13 \text{ TeV}$ with the ATLAS detector”, *Phys. Rev. D* **98** (2018) 032008, doi:10.1103/PhysRevD.98.032008, arXiv:1803.10178.
- [25] ATLAS Collaboration, “Search for supersymmetry in final states with charm jets and missing transverse momentum in 13 TeV pp collisions with the ATLAS detector”, *JHEP* **09** (2018) 050, doi:10.1007/JHEP09(2018)050, arXiv:1805.01649.
- [26] CMS Collaboration, “Search for top squark pair production in compressed-mass-spectrum scenarios in proton-proton collisions at $\sqrt{s} = 8 \text{ TeV}$ using the α_T variable”, *Phys. Lett. B* **767** (2017) 403, doi:10.1016/j.physletb.2017.02.007, arXiv:1605.08993.
- [27] CMS Collaboration, “Searches for pair production of third-generation squarks in $\sqrt{s} = 13 \text{ TeV}$ pp collisions”, *Eur. Phys. J. C* **77** (2017) 327, doi:10.1140/epjc/s10052-017-4853-2, arXiv:1612.03877.
- [28] CMS Collaboration, “Search for supersymmetry in the all-hadronic final state using top quark tagging in pp collisions at $\sqrt{s} = 13 \text{ TeV}$ ”, *Phys. Rev. D* **96** (2017) 012004, doi:10.1103/PhysRevD.96.012004, arXiv:1701.01954.
- [29] CMS Collaboration, “Search for top squark pair production in pp collisions at $\sqrt{s} = 13 \text{ TeV}$ using single lepton events”, *JHEP* **10** (2017) 019, doi:10.1007/JHEP10(2017)019, arXiv:1706.04402.

- [30] CMS Collaboration, “Search for direct production of supersymmetric partners of the top quark in the all-jets final state in proton-proton collisions at $\sqrt{s} = 13$ TeV”, *JHEP* **10** (2017) 005, doi:10.1007/JHEP10(2017)005, arXiv:1707.03316.
- [31] CMS Collaboration, “Search for the pair production of third-generation squarks with two-body decays to a bottom or charm quark and a neutralino in proton-proton collisions at $\sqrt{s} = 13$ TeV”, *Phys. Lett. B* **778** (2018) 263, doi:10.1016/j.physletb.2018.01.012, arXiv:1707.07274.
- [32] CMS Collaboration, “Search for supersymmetry in proton-proton collisions at 13 TeV using identified top quarks”, *Phys. Rev. D* **97** (2018) 012007, doi:10.1103/PhysRevD.97.012007, arXiv:1710.11188.
- [33] CMS Collaboration, “Search for top squarks and dark matter particles in opposite-charge dilepton final states at $\sqrt{s} = 13$ TeV”, *Phys. Rev. D* **97** (2018) 032009, doi:10.1103/PhysRevD.97.032009, arXiv:1711.00752.
- [34] CMS Collaboration, “Search for new physics in events with two soft oppositely charged leptons and missing transverse momentum in proton-proton collisions at $\sqrt{s} = 13$ TeV”, *Phys. Lett. B* **782** (2018) 440, doi:10.1016/j.physletb.2018.05.062, arXiv:1801.01846.
- [35] CMS Collaboration, “Search for top squarks decaying via four-body or chargino-mediated modes in single-lepton final states in proton-proton collisions at $\sqrt{s} = 13$ TeV”, *JHEP* **09** (2018) 065, doi:10.1007/JHEP09(2018)065, arXiv:1805.05784.
- [36] CMS Collaboration, “Search for pair-produced resonances decaying to quark pairs in proton-proton collisions at $\sqrt{s} = 13$ TeV”, *Phys. Rev. D* **98** (2018) 112014, doi:10.1103/PhysRevD.98.112014, arXiv:1808.03124.
- [37] CMS Collaboration, “Inclusive search for supersymmetry in pp collisions at $\sqrt{s} = 13$ TeV using razor variables and boosted object identification in zero and one lepton final states”, *JHEP* **03** (2019) 031, doi:10.1007/JHEP03(2019)031, arXiv:1812.06302.
- [38] CMS Collaboration, “Search for the pair production of light top squarks in the $e^{\pm}\mu^{\mp}$ final state in proton-proton collisions at $\sqrt{s} = 13$ TeV”, *JHEP* **03** (2019) 101, doi:10.1007/JHEP03(2019)101, arXiv:1901.01288.
- [39] CMS Collaboration, “The CMS experiment at the CERN LHC”, *JINST* **3** (2008) S08004, doi:10.1088/1748-0221/3/08/S08004.
- [40] CMS Collaboration, “The CMS trigger system”, *JINST* **12** (2017) P01020, doi:10.1088/1748-0221/12/01/P01020, arXiv:1609.02366.
- [41] CMS Collaboration, “CMS technical design report for the pixel detector upgrade”, Technical Report CERN-LHCC-2012-016, CMS-TDR-011, 2012. doi:10.2172/1151650.
- [42] J. Alwall et al., “The automated computation of tree-level and next-to-leading order differential cross sections, and their matching to parton shower simulations”, *JHEP* **07** (2014) 079, doi:10.1007/JHEP07(2014)079, arXiv:1405.0301.
- [43] P. Nason, “A new method for combining NLO QCD with shower Monte Carlo algorithms”, *JHEP* **11** (2004) 040, doi:10.1088/1126-6708/2004/11/040, arXiv:hep-ph/0409146.

-
- [44] S. Frixione, P. Nason, and C. Oleari, “Matching NLO QCD computations with parton shower simulations: the POWHEG method”, *JHEP* **11** (2007) 070, doi:10.1088/1126-6708/2007/11/070, arXiv:0709.2092.
- [45] S. Alioli, P. Nason, C. Oleari, and E. Re, “A general framework for implementing NLO calculations in shower Monte Carlo programs: the POWHEG BOX”, *JHEP* **06** (2010) 043, doi:10.1007/JHEP06(2010)043, arXiv:1002.2581.
- [46] E. Re, “Single-top Wt -channel production matched with parton showers using the POWHEG method”, *Eur. Phys. J. C* **71** (2011) 1547, doi:10.1140/epjc/s10052-011-1547-z, arXiv:1009.2450.
- [47] NNPDF Collaboration, “Unbiased global determination of parton distributions and their uncertainties at NNLO and at LO”, *Nucl. Phys. B* **855** (2012) 153, doi:10.1016/j.nuclphysb.2011.09.024, arXiv:1107.2652.
- [48] NNPDF Collaboration, “Parton distributions for the LHC Run II”, *JHEP* **04** (2015) 040, doi:10.1007/JHEP04(2015)040, arXiv:1410.8849.
- [49] NNPDF Collaboration, “Parton distributions from high-precision collider data”, *Eur. Phys. J. C* **77** (2017) 663, doi:10.1140/epjc/s10052-017-5199-5, arXiv:1706.00428.
- [50] T. Sjöstrand et al., “An introduction to PYTHIA 8.2”, *Comput. Phys. Commun.* **191** (2015) 159, doi:10.1016/j.cpc.2015.01.024, arXiv:1410.3012.
- [51] J. Alwall et al., “Comparative study of various algorithms for the merging of parton showers and matrix elements in hadronic collisions”, *Eur. Phys. J. C* **53** (2008) 473, doi:10.1140/epjc/s10052-007-0490-5, arXiv:0706.2569.
- [52] R. Frederix and S. Frixione, “Merging meets matching in MC@NLO”, *JHEP* **12** (2012) 061, doi:10.1007/JHEP12(2012)061, arXiv:1209.6215.
- [53] CMS Collaboration, “Event generator tunes obtained from underlying event and multiparton scattering measurements”, *Eur. Phys. J. C* **76** (2016) 155, doi:10.1140/epjc/s10052-016-3988-x, arXiv:1512.00815.
- [54] CMS Collaboration, “Extraction and validation of a new set of CMS PYTHIA8 tunes from underlying-event measurements”, (2019). arXiv:1903.12179. Submitted to *Eur. Phys. J. C*.
- [55] GEANT4 Collaboration, “GEANT4 — a simulation toolkit”, *Nucl. Instrum. Meth. A* **506** (2003) 250, doi:10.1016/S0168-9002(03)01368-8.
- [56] S. Abdullin et al., “The fast simulation of the CMS detector at LHC”, *J. Phys. Conf. Ser.* **331** (2011) 032049, doi:10.1088/1742-6596/331/3/032049.
- [57] A. Giammanco, “The Fast Simulation of the CMS Experiment”, *J. Phys. Conf. Ser.* **513** (2014) 022012, doi:10.1088/1742-6596/513/2/022012.
- [58] Y. Li and F. Petriello, “Combining QCD and electroweak corrections to dilepton production in FEWZ”, *Phys. Rev. D* **86** (2012) 094034, doi:10.1103/PhysRevD.86.094034, arXiv:1208.5967.

- [59] M. Aliev et al., “HATHOR: HAdronic Top and Heavy quarks crOss section calculatoR”, *Comput. Phys. Commun.* **182** (2011) 1034, doi:10.1016/j.cpc.2010.12.040, arXiv:1007.1327.
- [60] P. Kant et al., “HatHor for single top-quark production: Updated predictions and uncertainty estimates for single top-quark production in hadronic collisions”, *Comput. Phys. Commun.* **191** (2015) 74, doi:10.1016/j.cpc.2015.02.001, arXiv:1406.4403.
- [61] M. Beneke, P. Falgari, S. Klein, and C. Schwinn, “Hadronic top-quark pair production with NNLL threshold resummation”, *Nucl. Phys. B* **855** (2012) 695, doi:10.1016/j.nuclphysb.2011.10.021, arXiv:1109.1536.
- [62] M. Cacciari et al., “Top-pair production at hadron colliders with next-to-next-to-leading logarithmic soft-gluon resummation”, *Phys. Lett. B* **710** (2012) 612, doi:10.1016/j.physletb.2012.03.013, arXiv:1111.5869.
- [63] M. Czakon and A. Mitov, “Top++: A Program for the Calculation of the Top-Pair Cross-Section at Hadron Colliders”, *Comput. Phys. Commun.* **185** (2014) 2930, doi:10.1016/j.cpc.2014.06.021, arXiv:1112.5675.
- [64] P. Bärnreuther, M. Czakon, and A. Mitov, “Percent level precision physics at the tevatron: First genuine NNLO QCD corrections to $q\bar{q} \rightarrow t\bar{t} + X$ ”, *Phys. Rev. Lett.* **109** (2012) 132001, doi:10.1103/PhysRevLett.109.132001, arXiv:1204.5201.
- [65] M. Czakon and A. Mitov, “NNLO corrections to top-pair production at hadron colliders: the all-fermionic scattering channels”, *JHEP* **12** (2012) 054, doi:10.1007/JHEP12(2012)054, arXiv:1207.0236.
- [66] M. Czakon and A. Mitov, “NNLO corrections to top pair production at hadron colliders: the quark-gluon reaction”, *JHEP* **01** (2013) 080, doi:10.1007/JHEP01(2013)080, arXiv:1210.6832.
- [67] M. Czakon, P. Fiedler, and A. Mitov, “Total top-quark pair-production cross section at hadron colliders through $O(\alpha_s^4)$ ”, *Phys. Rev. Lett.* **110** (2013) 252004, doi:10.1103/PhysRevLett.110.252004, arXiv:1303.6254.
- [68] W. Beenakker, R. Hopker, M. Spira, and P. M. Zerwas, “Squark and gluino production at hadron colliders”, *Nucl. Phys. B* **492** (1997) 51, doi:10.1016/S0550-3213(97)80027-2, arXiv:hep-ph/9610490.
- [69] A. Kulesza and L. Motyka, “Threshold resummation for squark-antisquark and gluino-pair production at the LHC”, *Phys. Rev. Lett.* **102** (2009) 111802, doi:10.1103/PhysRevLett.102.111802, arXiv:0807.2405.
- [70] A. Kulesza and L. Motyka, “Soft gluon resummation for the production of gluino-gluino and squark-antisquark pairs at the LHC”, *Phys. Rev. D* **80** (2009) 095004, doi:10.1103/PhysRevD.80.095004, arXiv:0905.4749.
- [71] W. Beenakker et al., “Soft-gluon resummation for squark and gluino hadroproduction”, *JHEP* **12** (2009) 041, doi:10.1088/1126-6708/2009/12/041, arXiv:0909.4418.
- [72] W. Beenakker et al., “Squark and Gluino Hadroproduction”, *Int. J. Mod. Phys. A* **26** (2011) 2637, doi:10.1142/S0217751X11053560, arXiv:1105.1110.

-
- [73] C. Borschensky et al., “Squark and gluino production cross sections in pp collisions at $\sqrt{s} = 13, 14, 33$ and 100 TeV”, *Eur. Phys. J. C* **74** (2014) 3174, doi:10.1140/epjc/s10052-014-3174-y, arXiv:1407.5066.
- [74] W. Beenakker et al., “NNLL-fast: predictions for coloured supersymmetric particle production at the LHC with threshold and Coulomb resummation”, *JHEP* **12** (2016) 133, doi:10.1007/JHEP12(2016)133, arXiv:1607.07741.
- [75] CMS Collaboration, “Particle-flow reconstruction and global event description with the CMS detector”, *JINST* **12** (2017) P10003, doi:10.1088/1748-0221/12/10/P10003, arXiv:1706.04965.
- [76] M. Cacciari and G. P. Salam, “Dispelling the N^3 myth for the k_T jet-finder”, *Phys. Lett. B* **641** (2006) 57, doi:10.1016/j.physletb.2006.08.037, arXiv:hep-ph/0512210.
- [77] M. Cacciari, G. P. Salam, and G. Soyez, “The anti- k_T jet clustering algorithm”, *JHEP* **04** (2008) 063, doi:10.1088/1126-6708/2008/04/063, arXiv:0802.1189.
- [78] M. Cacciari, G. P. Salam, and G. Soyez, “FastJet user manual”, *Eur. Phys. J. C* **72** (2012) 1896, doi:10.1140/epjc/s10052-012-1896-2, arXiv:1111.6097.
- [79] CMS Collaboration, “Missing transverse energy performance of the CMS detector”, *JINST* **6** (2011) P09001, doi:10.1088/1748-0221/6/09/P09001, arXiv:1106.5048.
- [80] CMS Collaboration, “Performance of electron reconstruction and selection with the CMS detector in proton-proton collisions at $\sqrt{s} = 8$ TeV”, *JINST* **10** (2015) P06005, doi:10.1088/1748-0221/10/06/P06005, arXiv:1502.02701.
- [81] CMS Collaboration, “Performance of the CMS muon detector and muon reconstruction with proton-proton collisions at $\sqrt{s} = 13$ TeV”, *JINST* **13** (2018) P06015, doi:10.1088/1748-0221/13/06/P06015, arXiv:1804.04528.
- [82] M. Cacciari and G. P. Salam, “Pileup subtraction using jet areas”, *Phys. Lett. B* **659** (2008) 119, doi:10.1016/j.physletb.2007.09.077, arXiv:0707.1378.
- [83] CMS Collaboration, “Jet algorithms performance in 13 TeV data”, CMS Physics Analysis Summary CMS-PAS-JME-16-003, 2017.
- [84] CMS Collaboration, “Jet energy scale and resolution in the CMS experiment in pp collisions at 8 TeV”, *JINST* **12** (2017) P02014, doi:10.1088/1748-0221/12/02/P02014, arXiv:1607.03663.
- [85] CMS Collaboration, “Jet energy scale and resolution performance with 13 TeV data collected by CMS in 2016”, Detector Performance Report CMS-DP-2018-028, 2018.
- [86] CMS Collaboration, “Identification of heavy-flavour jets with the CMS detector in pp collisions at 13 TeV”, *JINST* **13** (2018) P05011, doi:10.1088/1748-0221/13/05/P05011, arXiv:1712.07158.
- [87] CMS Collaboration, “Measurement of $B\bar{B}$ Angular Correlations based on Secondary Vertex Reconstruction at $\sqrt{s} = 7$ TeV”, *JHEP* **03** (2011) 136, doi:10.1007/JHEP03(2011)136, arXiv:1102.3194.

- [88] Y. Ganin and V. Lempitsky, “Unsupervised domain adaptation by backpropagation”, 2014. <https://arxiv.org/pdf/1409.7495v2.pdf>.
- [89] CMS Collaboration, “Machine learning-based identification of highly Lorentz-boosted hadronically decaying particles at the CMS experiment”, CMS Physics Analysis Summary CMS-PAS-JME-18-002, 2019.
- [90] M. L. Graesser and J. Shelton, “Hunting mixed top squark decays”, *Phys. Rev. Lett.* **111** (2013) 121802, doi:10.1103/PhysRevLett.111.121802, arXiv:1212.4495.
- [91] CMS Collaboration, “Measurement of the cross section for top quark pair production in association with a W or Z boson in proton-proton collisions at $\sqrt{s} = 13$ TeV”, *JHEP* **08** (2018) 011, doi:10.1007/JHEP08(2018)011, arXiv:1711.02547.
- [92] S. Catani, D. de Florian, M. Grazzini, and P. Nason, “Soft-gluon resummation for Higgs boson production at hadron colliders”, *JHEP* **07** (2003) 028, doi:10.1088/1126-6708/2003/07/028, arXiv:hep-ph/0306211.
- [93] M. Cacciari et al., “The $t\bar{t}$ cross-section at 1.8 TeV and 1.96 TeV: a study of the systematics due to parton densities and scale dependence”, *JHEP* **04** (2004) 068, doi:10.1088/1126-6708/2004/04/068, arXiv:hep-ph/0303085.
- [94] J. Butterworth et al., “PDF4LHC recommendations for LHC Run II”, *J. Phys. G* **43** (2016) 023001, doi:10.1088/0954-3899/43/2/023001, arXiv:1510.03865.
- [95] T. Junk, “Confidence level computation for combining searches with small statistics”, *Nucl. Instrum. Meth. A* **434** (1999) 435, doi:10.1016/S0168-9002(99)00498-2, arXiv:hep-ex/9902006.
- [96] A. L. Read, “Presentation of search results: the CL_S technique”, *J. Phys. G* **28** (2002) 2693, doi:10.1088/0954-3899/28/10/313.
- [97] G. Cowan, K. Cranmer, E. Gross, and O. Vitells, “Asymptotic formulae for likelihood-based tests of new physics”, *Eur. Phys. J. C* **71** (2011) 1554, doi:10.1140/epjc/s10052-011-1554-0, arXiv:1007.1727. [Erratum: 10.1140/epjc/s10052-013-2501-z].
- [98] ATLAS and CMS Collaborations, and the LHC Higgs Combination Group, “Procedure for the LHC Higgs boson search combination in summer 2011”, ATLAS/CMS joint note ATL-PHYS-PUB-2011-011, CMS-NOTE-2011-005, 2011.

A The CMS Collaboration

Yerevan Physics Institute, Yerevan, Armenia

A.M. Sirunyan[†], A. Tumasyan

Institut für Hochenergiephysik, Wien, Austria

W. Adam, F. Ambrogio, T. Bergauer, J. Brandstetter, M. Dragicevic, J. Erö, A. Escalante Del Valle, M. Flechl, R. Frühwirth¹, M. Jeitler¹, N. Krammer, I. Krätschmer, D. Liko, T. Madlener, I. Mikulec, N. Rad, J. Schieck¹, R. Schöfbeck, M. Spanring, D. Spitzbart, W. Waltenberger, C.-E. Wulz¹, M. Zarucki

Institute for Nuclear Problems, Minsk, Belarus

V. Drugakov, V. Mossolov, J. Suarez Gonzalez

Universiteit Antwerpen, Antwerpen, Belgium

M.R. Darwish, E.A. De Wolf, D. Di Croce, X. Janssen, A. Lelek, M. Pieters, H. Rejeb Sfar, H. Van Haevermaet, P. Van Mechelen, S. Van Putte, N. Van Remortel

Vrije Universiteit Brussel, Brussel, Belgium

F. Blekman, E.S. Bols, S.S. Chhibra, J. D'Hondt, J. De Clercq, D. Lontkovskyi, S. Lowette, I. Marchesini, S. Moortgat, Q. Python, K. Skovpen, S. Tavernier, W. Van Doninck, P. Van Mulders

Université Libre de Bruxelles, Bruxelles, Belgium

D. Beghin, B. Bilin, H. Brun, B. Clerbaux, G. De Lentdecker, H. Delannoy, B. Dorney, L. Favart, A. Grebenyuk, A.K. Kalsi, A. Popov, N. Postiau, E. Starling, L. Thomas, C. Vander Velde, P. Vanlaer, D. Vannerom

Ghent University, Ghent, Belgium

T. Cornelis, D. Dobur, I. Khvastunov², M. Niedziela, C. Roskas, M. Tytgat, W. Verbeke, B. Vermassen, M. Vit

Université Catholique de Louvain, Louvain-la-Neuve, Belgium

O. Bondu, G. Bruno, C. Caputo, P. David, C. Delaere, M. Delcourt, A. Giammanco, V. Lemaitre, J. Prisciandaro, A. Saggio, M. Vidal Marono, P. Vischia, J. Zobec

Centro Brasileiro de Pesquisas Físicas, Rio de Janeiro, Brazil

F.L. Alves, G.A. Alves, G. Correia Silva, C. Hensel, A. Moraes, P. Rebello Teles

Universidade do Estado do Rio de Janeiro, Rio de Janeiro, Brazil

E. Belchior Batista Das Chagas, W. Carvalho, J. Chinellato³, E. Coelho, E.M. Da Costa, G.G. Da Silveira⁴, D. De Jesus Damiao, C. De Oliveira Martins, S. Fonseca De Souza, L.M. Huertas Guativa, H. Malbouisson, J. Martins⁵, D. Matos Figueiredo, M. Medina Jaime⁶, M. Melo De Almeida, C. Mora Herrera, L. Mundim, H. Nogima, W.L. Prado Da Silva, L.J. Sanchez Rosas, A. Santoro, A. Sznajder, M. Thiel, E.J. Tonelli Manganote³, F. Torres Da Silva De Araujo, A. Vilela Pereira

Universidade Estadual Paulista ^a, Universidade Federal do ABC ^b, São Paulo, Brazil

C.A. Bernardes^a, L. Calligaris^a, T.R. Fernandez Perez Tomei^a, E.M. Gregores^b, D.S. Lemos, P.G. Mercadante^b, S.F. Novaes^a, SandraS. Padula^a

Institute for Nuclear Research and Nuclear Energy, Bulgarian Academy of Sciences, Sofia, Bulgaria

A. Aleksandrov, G. Antchev, R. Hadjiiska, P. Iaydjiev, M. Misheva, M. Rodozov, M. Shopova, G. Sultanov

University of Sofia, Sofia, Bulgaria

M. Bonchev, A. Dimitrov, T. Ivanov, L. Litov, B. Pavlov, P. Petkov

Beihang University, Beijing, China

W. Fang⁷, X. Gao⁷, L. Yuan

Institute of High Energy Physics, Beijing, China

G.M. Chen, H.S. Chen, M. Chen, C.H. Jiang, D. Leggat, H. Liao, Z. Liu, A. Spiezia, J. Tao, E. Yazgan, H. Zhang, S. Zhang⁸, J. Zhao

State Key Laboratory of Nuclear Physics and Technology, Peking University, Beijing, China

A. Agapitos, Y. Ban, G. Chen, A. Levin, J. Li, L. Li, Q. Li, Y. Mao, S.J. Qian, D. Wang, Q. Wang

Tsinghua University, Beijing, China

M. Ahmad, Z. Hu, Y. Wang

Zhejiang University, Hangzhou, China

M. Xiao

Universidad de Los Andes, Bogota, Colombia

C. Avila, A. Cabrera, C. Florez, C.F. González Hernández, M.A. Segura Delgado

Universidad de Antioquia, Medellin, Colombia

J. Mejia Guisao, J.D. Ruiz Alvarez, C.A. Salazar González, N. Vanegas Arbelaez

University of Split, Faculty of Electrical Engineering, Mechanical Engineering and Naval Architecture, Split, Croatia

D. Giljanović, N. Godinovic, D. Lelas, I. Puljak, T. Sculac

University of Split, Faculty of Science, Split, Croatia

Z. Antunovic, M. Kovac

Institute Rudjer Boskovic, Zagreb, Croatia

V. Brigljevic, D. Ferencek, K. Kadija, B. Mesic, M. Roguljic, A. Starodumov⁹, T. Susa

University of Cyprus, Nicosia, Cyprus

M.W. Ather, A. Attikis, E. Erodotou, A. Ioannou, M. Kolosova, S. Konstantinou, G. Mavromanolakis, J. Mousa, C. Nicolaou, F. Ptochos, P.A. Razis, H. Rykaczewski, D. Tsiakkouri

Charles University, Prague, Czech Republic

M. Finger¹⁰, M. Finger Jr.¹⁰, A. Kveton, J. Tomsa

Escuela Politecnica Nacional, Quito, Ecuador

E. Ayala

Universidad San Francisco de Quito, Quito, Ecuador

E. Carrera Jarrin

Academy of Scientific Research and Technology of the Arab Republic of Egypt, Egyptian Network of High Energy Physics, Cairo, Egypt

H. Abdalla¹¹, S. Khalil¹²

National Institute of Chemical Physics and Biophysics, Tallinn, Estonia

S. Bhowmik, A. Carvalho Antunes De Oliveira, R.K. Dewanjee, K. Ehataht, M. Kadastik, M. Raidal, C. Veelken

Department of Physics, University of Helsinki, Helsinki, Finland

P. Eerola, L. Forthomme, H. Kirschenmann, K. Osterberg, M. Voutilainen

Helsinki Institute of Physics, Helsinki, Finland

F. Garcia, J. Havukainen, J.K. Heikkilä, V. Karimäki, M.S. Kim, R. Kinnunen, T. Lampén, K. Lassila-Perini, S. Laurila, S. Lehti, T. Lindén, P. Luukka, T. Mäenpää, H. Siikonen, E. Tuominen, J. Tuominiemi

Lappeenranta University of Technology, Lappeenranta, Finland

T. Tuuva

IRFU, CEA, Université Paris-Saclay, Gif-sur-Yvette, France

M. Besancon, F. Couderc, M. Dejardin, D. Denegri, B. Fabbro, J.L. Faure, F. Ferri, S. Ganjour, A. Givernaud, P. Gras, G. Hamel de Monchenault, P. Jarry, C. Leloup, B. Lenzi, E. Locci, J. Malcles, J. Rander, A. Rosowsky, M.Ö. Sahin, A. Savoy-Navarro¹³, M. Titov, G.B. Yu

Laboratoire Leprince-Ringuet, CNRS/IN2P3, Ecole Polytechnique, Institut Polytechnique de Paris

S. Ahuja, C. Amendola, F. Beaudette, P. Busson, C. Charlot, B. Diab, G. Falmagne, R. Granier de Cassagnac, I. Kucher, A. Lobanov, C. Martin Perez, M. Nguyen, C. Ochando, P. Paganini, J. Rembser, R. Salerno, J.B. Sauvan, Y. Sirois, A. Zabi, A. Zghiche

Université de Strasbourg, CNRS, IPHC UMR 7178, Strasbourg, France

J.-L. Agram¹⁴, J. Andrea, D. Bloch, G. Bourgatte, J.-M. Brom, E.C. Chabert, C. Collard, E. Conte¹⁴, J.-C. Fontaine¹⁴, D. Gelé, U. Goerlach, M. Jansová, A.-C. Le Bihan, N. Tonon, P. Van Hove

Centre de Calcul de l'Institut National de Physique Nucleaire et de Physique des Particules, CNRS/IN2P3, Villeurbanne, France

S. Gadrat

Université de Lyon, Université Claude Bernard Lyon 1, CNRS-IN2P3, Institut de Physique Nucléaire de Lyon, Villeurbanne, France

S. Beauceron, C. Bernet, G. Boudoul, C. Camen, A. Carle, N. Chanon, R. Chierici, D. Contardo, P. Depasse, H. El Mamouni, J. Fay, S. Gascon, M. Gouzevitch, B. Ille, Sa. Jain, F. Lagarde, I.B. Laktineh, H. Lattaud, A. Lesauvage, M. Lethuillier, L. Mirabito, S. Perries, V. Sordini, L. Torterotot, G. Touquet, M. Vander Donckt, S. Viret

Georgian Technical University, Tbilisi, Georgia

G. Adamov

Tbilisi State University, Tbilisi, Georgia

Z. Tsamalaidze¹⁰

RWTH Aachen University, I. Physikalisches Institut, Aachen, Germany

C. Autermann, L. Feld, M.K. Kiesel, K. Klein, M. Lipinski, D. Meuser, A. Pauls, M. Preuten, M.P. Rauch, J. Schulz, M. Teroerde, B. Wittmer

RWTH Aachen University, III. Physikalisches Institut A, Aachen, Germany

M. Erdmann, B. Fischer, S. Ghosh, T. Hebbeker, K. Hoepfner, H. Keller, L. Mastrolorenzo, M. Merschmeyer, A. Meyer, P. Millet, G. Mocellin, S. Mondal, S. Mukherjee, D. Noll, A. Novak, T. Pook, A. Pozdnyakov, T. Quast, M. Radziej, Y. Rath, H. Reithler, J. Roemer, A. Schmidt, S.C. Schuler, A. Sharma, S. Wiedenbeck, S. Zaleski

RWTH Aachen University, III. Physikalisches Institut B, Aachen, Germany

G. Flügge, W. Haj Ahmad¹⁵, O. Hlushchenko, T. Kress, T. Müller, A. Nowack, C. Pistone, O. Pooth, D. Roy, H. Sert, A. Stahl¹⁶

Deutsches Elektronen-Synchrotron, Hamburg, Germany

M. Aldaya Martin, P. Asmuss, I. Babounikau, H. Bakhshiansohi, K. Beernaert, O. Behnke, A. Bermúdez Martínez, D. Bertsche, A.A. Bin Anuar, K. Borras¹⁷, V. Botta, A. Campbell, A. Cardini, P. Connor, S. Consuegra Rodríguez, C. Contreras-Campana, V. Danilov, A. De Wit, M.M. Defranchis, C. Diez Pardos, D. Domínguez Damiani, G. Eckerlin, D. Eckstein, T. Eichhorn, A. Elwood, E. Eren, E. Gallo¹⁸, A. Geiser, A. Grohsjean, M. Guthoff, M. Haranko, A. Harb, A. Jafari, N.Z. Jomhari, H. Jung, A. Kasem¹⁷, M. Kasemann, H. Kaveh, J. Keaveney, C. Kleinwort, J. Knolle, D. Krücker, W. Lange, T. Lenz, J. Lidrych, K. Lipka, W. Lohmann¹⁹, R. Mankel, I.-A. Melzer-Pellmann, A.B. Meyer, M. Meyer, M. Missiroli, G. Mittag, J. Mnich, A. Mussgiller, V. Myronenko, D. Pérez Adán, S.K. Pflitsch, D. Pitzl, A. Raspereza, A. Saibel, M. Savitskiy, V. Scheurer, P. Schütze, C. Schwanenberger, R. Shevchenko, A. Singh, H. Tholen, O. Turkot, A. Vagnerini, M. Van De Klundert, R. Walsh, Y. Wen, K. Wichmann, C. Wissing, O. Zenaiev, R. Zlebcik

University of Hamburg, Hamburg, Germany

R. Aggleton, S. Bein, L. Benato, A. Benecke, V. Blobel, T. Dreyer, A. Ebrahimi, F. Feindt, A. Fröhlich, C. Garbers, E. Garutti, D. Gonzalez, P. Gunnellini, J. Haller, A. Hinzmann, A. Karavdina, G. Kasieczka, R. Klanner, R. Kogler, N. Kovalchuk, S. Kurz, V. Kutzner, J. Lange, T. Lange, A. Malara, J. Multhaupt, C.E.N. Niemeyer, A. Perieanu, A. Reimers, O. Rieger, C. Scharf, P. Schleper, S. Schumann, J. Schwandt, J. Sonneveld, H. Stadie, G. Steinbrück, F.M. Stober, B. Vormwald, I. Zoi

Karlsruher Institut fuer Technologie, Karlsruhe, Germany

M. Akbiyik, C. Barth, M. Baselga, S. Baur, T. Berger, E. Butz, R. Caspart, T. Chwalek, W. De Boer, A. Dierlamm, K. El Morabit, N. Faltermann, M. Giffels, P. Goldenzweig, A. Gottmann, M.A. Harrendorf, F. Hartmann¹⁶, U. Husemann, S. Kudella, S. Mitra, M.U. Mozer, D. Müller, Th. Müller, M. Musich, A. Nürnberg, G. Quast, K. Rabbertz, M. Schröder, I. Shvetsov, H.J. Simonis, R. Ulrich, M. Wassmer, M. Weber, C. Wöhrmann, R. Wolf

Institute of Nuclear and Particle Physics (INPP), NCSR Demokritos, Aghia Paraskevi, Greece

G. Anagnostou, P. Asenov, G. Daskalakis, T. Geralis, A. Kyriakis, D. Loukas, G. Paspalaki

National and Kapodistrian University of Athens, Athens, Greece

M. Diamantopoulou, G. Karathanasis, P. Kontaxakis, A. Manousakis-katsikakis, A. Panagiotou, I. Papavergou, N. Saoulidou, A. Stakia, K. Theofilatos, K. Vellidis, E. Vourliotis

National Technical University of Athens, Athens, Greece

G. Bakas, K. Kousouris, I. Papakrivopoulos, G. Tsipolitis

University of Ioánnina, Ioánnina, Greece

I. Evangelou, C. Foudas, P. Giannelis, P. Katsoulis, P. Kokkas, S. Mallios, K. Manitará, N. Manthos, I. Papadopoulos, J. Strologas, F.A. Triantis, D. Tsitsonis

MTA-ELTE Lendület CMS Particle and Nuclear Physics Group, Eötvös Loránd University, Budapest, Hungary

M. Bartók²⁰, R. Chudasama, M. Csanad, P. Major, K. Mandal, A. Mehta, M.I. Nagy, G. Pasztor, O. Surányi, G.I. Veres

Wigner Research Centre for Physics, Budapest, Hungary

G. Bencze, C. Hajdu, D. Horvath²¹, F. Sikler, T. Vámi, V. Veszpremi, G. Vesztergombi[†]

Institute of Nuclear Research ATOMKI, Debrecen, Hungary

N. Beni, S. Czellar, J. Karancsi²⁰, A. Makovec, J. Molnar, Z. Szillasi

Institute of Physics, University of Debrecen, Debrecen, Hungary

P. Raics, D. Teyssier, Z.L. Trocsanyi, B. Ujvari

Eszterhazy Karoly University, Karoly Robert Campus, Gyongyos, Hungary

T. Csorgo, W.J. Metzger, F. Nemes, T. Novak

Indian Institute of Science (IISc), Bangalore, India

S. Choudhury, J.R. Komaragiri, P.C. Tiwari

National Institute of Science Education and Research, HBNI, Bhubaneswar, IndiaS. Bahinipati²³, C. Kar, G. Kole, P. Mal, V.K. Muraleedharan Nair Bindhu, A. Nayak²⁴, D.K. Sahoo²³, S.K. Swain**Panjab University, Chandigarh, India**

S. Bansal, S.B. Beri, V. Bhatnagar, S. Chauhan, R. Chawla, N. Dhingra, R. Gupta, A. Kaur, M. Kaur, S. Kaur, P. Kumari, M. Lohan, M. Meena, K. Sandeep, S. Sharma, J.B. Singh, A.K. Viridi

University of Delhi, Delhi, India

A. Bhardwaj, B.C. Choudhary, R.B. Garg, M. Gola, S. Keshri, Ashok Kumar, M. Naimuddin, P. Priyanka, K. Ranjan, Aashaq Shah, R. Sharma

Saha Institute of Nuclear Physics, HBNI, Kolkata, IndiaR. Bhardwaj²⁵, M. Bharti²⁵, R. Bhattacharya, S. Bhattacharya, U. Bhawandeep²⁵, D. Bhowmik, S. Dutta, S. Ghosh, B. Gomber²⁶, M. Maity²⁷, K. Mondal, S. Nandan, A. Purohit, P.K. Rout, G. Saha, S. Sarkar, T. Sarkar²⁷, M. Sharan, B. Singh²⁵, S. Thakur²⁵**Indian Institute of Technology Madras, Madras, India**

P.K. Behera, P. Kalbhor, A. Muhammad, P.R. Pujahari, A. Sharma, A.K. Sikdar

Bhabha Atomic Research Centre, Mumbai, India

D. Dutta, V. Jha, V. Kumar, D.K. Mishra, P.K. Netrakanti, L.M. Pant, P. Shukla

Tata Institute of Fundamental Research-A, Mumbai, India

T. Aziz, M.A. Bhat, S. Dugad, G.B. Mohanty, N. Sur, RavindraKumar Verma

Tata Institute of Fundamental Research-B, Mumbai, India

S. Banerjee, S. Bhattacharya, S. Chatterjee, P. Das, M. Guchait, S. Karmakar, S. Kumar, G. Majumder, K. Mazumdar, N. Sahoo, S. Sawant

Indian Institute of Science Education and Research (IISER), Pune, India

S. Dube, V. Hegde, B. Kansal, A. Kapoor, K. Kothekar, S. Pandey, A. Rane, A. Rastogi, S. Sharma

Institute for Research in Fundamental Sciences (IPM), Tehran, IranS. Chenarani²⁸, E. Eskandari Tadavani, S.M. Etesami²⁸, M. Khakzad, M. Mohammadi Najafabadi, M. Naseri, F. Rezaei Hosseinabadi**University College Dublin, Dublin, Ireland**

M. Felcini, M. Grunewald

INFN Sezione di Bari ^a, Università di Bari ^b, Politecnico di Bari ^c, Bari, ItalyM. Abbrescia^{a,b}, R. Aly^{a,b,29}, C. Calabria^{a,b}, A. Colaleo^a, D. Creanza^{a,c}, L. Cristella^{a,b}, N. De Filippis^{a,c}, M. De Palma^{a,b}, A. Di Florio^{a,b}, W. Elmetenawee^{a,b}, L. Fiore^a, A. Gelmi^{a,b}, G. Iaselli^{a,c}, M. Ince^{a,b}, S. Lezki^{a,b}, G. Maggi^{a,c}, M. Maggi^a, G. Miniello^{a,b}, S. My^{a,b}, S. Nuzzo^{a,b}, A. Pompili^{a,b}, G. Pugliese^{a,c}, R. Radogna^a, A. Ranieri^a, G. Selvaggi^{a,b}, L. Silvestris^a, F.M. Simone^{a,b}, R. Venditti^a, P. Verwilligen^a

INFN Sezione di Bologna ^a, Università di Bologna ^b, Bologna, Italy

G. Abbiendi^a, C. Battilana^{a,b}, D. Bonacorsi^{a,b}, L. Borgonovi^{a,b}, S. Braibant-Giacomelli^{a,b}, R. Campanini^{a,b}, P. Capiluppi^{a,b}, A. Castro^{a,b}, F.R. Cavallo^a, C. Ciocca^a, G. Codispoti^{a,b}, M. Cuffiani^{a,b}, G.M. Dallavalle^a, F. Fabbri^a, A. Fanfani^{a,b}, E. Fontanesi^{a,b}, P. Giacomelli^a, C. Grandi^a, L. Guiducci^{a,b}, F. Iemmi^{a,b}, S. Lo Meo^{a,30}, S. Marcellini^a, G. Masetti^a, F.L. Navarria^{a,b}, A. Perrotta^a, F. Primavera^{a,b}, A.M. Rossi^{a,b}, T. Rovelli^{a,b}, G.P. Siroli^{a,b}, N. Tosi^a

INFN Sezione di Catania ^a, Università di Catania ^b, Catania, Italy

S. Albergo^{a,b,31}, S. Costa^{a,b}, A. Di Mattia^a, R. Potenza^{a,b}, A. Tricomi^{a,b,31}, C. Tuve^{a,b}

INFN Sezione di Firenze ^a, Università di Firenze ^b, Firenze, Italy

G. Barbagli^a, A. Cassese, R. Ceccarelli, V. Ciulli^{a,b}, C. Civinini^a, R. D'Alessandro^{a,b}, E. Focardi^{a,b}, G. Latino^{a,b}, P. Lenzi^{a,b}, M. Meschini^a, S. Paoletti^a, G. Sguazzoni^a, L. Viliani^a

INFN Laboratori Nazionali di Frascati, Frascati, Italy

L. Benussi, S. Bianco, D. Piccolo

INFN Sezione di Genova ^a, Università di Genova ^b, Genova, Italy

M. Bozzo^{a,b}, F. Ferro^a, R. Mulargia^{a,b}, E. Robutti^a, S. Tosi^{a,b}

INFN Sezione di Milano-Bicocca ^a, Università di Milano-Bicocca ^b, Milano, Italy

A. Benaglia^a, A. Beschi^{a,b}, F. Brivio^{a,b}, V. Ciriolo^{a,b,16}, S. Di Guida^{a,b,16}, M.E. Dinardo^{a,b}, P. Dini^a, S. Gennai^a, A. Ghezzi^{a,b}, P. Govoni^{a,b}, L. Guzzi^{a,b}, M. Malberti^a, S. Malvezzi^a, D. Menasce^a, F. Monti^{a,b}, L. Moroni^a, M. Paganoni^{a,b}, D. Pedrini^a, S. Ragazzi^{a,b}, T. Tabarelli de Fatis^{a,b}, D. Zuolo^{a,b}

INFN Sezione di Napoli ^a, Università di Napoli 'Federico II' ^b, Napoli, Italy, Università della Basilicata ^c, Potenza, Italy, Università G. Marconi ^d, Roma, Italy

S. Buontempo^a, N. Cavallo^{a,c}, A. De Iorio^{a,b}, A. Di Crescenzo^{a,b}, F. Fabozzi^{a,c}, F. Fienga^a, G. Galati^a, A.O.M. Iorio^{a,b}, L. Lista^{a,b}, S. Meola^{a,d,16}, P. Paolucci^{a,16}, B. Rossi^a, C. Sciacca^{a,b}, E. Voevodina^{a,b}

INFN Sezione di Padova ^a, Università di Padova ^b, Padova, Italy, Università di Trento ^c, Trento, Italy

P. Azzi^a, N. Bacchetta^a, D. Bisello^{a,b}, A. Boletti^{a,b}, A. Bragagnolo^{a,b}, R. Carlin^{a,b}, P. Checchia^a, P. De Castro Manzano^a, T. Dorigo^a, U. Dosselli^a, F. Gasparini^{a,b}, U. Gasparini^{a,b}, A. Gozzelino^a, S.Y. Hoh^{a,b}, P. Lujan^a, M. Margoni^{a,b}, A.T. Meneguzzo^{a,b}, J. Pazzini^{a,b}, M. Presilla^b, P. Ronchese^{a,b}, R. Rossin^{a,b}, F. Simonetto^{a,b}, A. Tiko^a, M. Tosi^{a,b}, M. Zanetti^{a,b}, P. Zotto^{a,b}, G. Zumerle^{a,b}

INFN Sezione di Pavia ^a, Università di Pavia ^b, Pavia, Italy

A. Braghieri^a, D. Fiorina^{a,b}, P. Montagna^{a,b}, S.P. Ratti^{a,b}, V. Re^a, M. Ressegotti^{a,b}, C. Riccardi^{a,b}, P. Salvini^a, I. Vai^a, P. Vitulo^{a,b}

INFN Sezione di Perugia ^a, Università di Perugia ^b, Perugia, Italy

M. Biasini^{a,b}, G.M. Bilei^a, D. Ciangottini^{a,b}, L. Fanò^{a,b}, P. Lariccia^{a,b}, R. Leonardi^{a,b}, E. Manoni^a, G. Mantovani^{a,b}, V. Mariani^{a,b}, M. Menichelli^a, A. Rossi^{a,b}, A. Santocchia^{a,b}, D. Spiga^a

INFN Sezione di Pisa ^a, Università di Pisa ^b, Scuola Normale Superiore di Pisa ^c, Pisa, Italy

K. Androsov^a, P. Azzurri^a, G. Bagliesi^a, V. Bertacchi^{a,c}, L. Bianchini^a, T. Boccali^a, R. Castaldi^a, M.A. Ciocci^{a,b}, R. Dell'Orso^a, S. Donato^a, G. Fedi^a, L. Giannini^{a,c}, A. Giassi^a, M.T. Grippo^a, F. Ligabue^{a,c}, E. Manca^{a,c}, G. Mandorli^{a,c}, A. Messineo^{a,b}, F. Palla^a, A. Rizzi^{a,b}, G. Rolandi³², S. Roy Chowdhury, A. Scribano^a, P. Spagnolo^a, R. Tenchini^a, G. Tonelli^{a,b}, N. Turini, A. Venturi^a, P.G. Verdini^a

INFN Sezione di Roma ^a, Sapienza Università di Roma ^b, Rome, Italy

F. Cavallari^a, M. Cipriani^{a,b}, D. Del Re^{a,b}, E. Di Marco^{a,b}, M. Diemoz^a, E. Longo^{a,b}, P. Meridiani^a, G. Organtini^{a,b}, F. Pandolfi^a, R. Paramatti^{a,b}, C. Quaranta^{a,b}, S. Rahatlou^{a,b}, C. Rovelli^a, F. Santanastasio^{a,b}, L. Soffi^{a,b}

INFN Sezione di Torino ^a, Università di Torino ^b, Torino, Italy, Università del Piemonte Orientale ^c, Novara, Italy

N. Amapane^{a,b}, R. Arcidiacono^{a,c}, S. Argiro^{a,b}, M. Arneodo^{a,c}, N. Bartosik^a, R. Bellan^{a,b}, A. Bellora, C. Biino^a, A. Cappati^{a,b}, N. Cartiglia^a, S. Cometti^a, M. Costa^{a,b}, R. Covarelli^{a,b}, N. Demaria^a, B. Kiani^{a,b}, F. Legger, C. Mariotti^a, S. Maselli^a, E. Migliore^{a,b}, V. Monaco^{a,b}, E. Monteil^{a,b}, M. Monteno^a, M.M. Obertino^{a,b}, G. Ortona^{a,b}, L. Pacher^{a,b}, N. Pastrone^a, M. Pelliccioni^a, G.L. Pinna Angioni^{a,b}, A. Romero^{a,b}, M. Ruspa^{a,c}, R. Salvatico^{a,b}, V. Sola^a, A. Solano^{a,b}, D. Soldi^{a,b}, A. Staiano^a, D. Trocino^{a,b}

INFN Sezione di Trieste ^a, Università di Trieste ^b, Trieste, Italy

S. Belforte^a, V. Candelise^{a,b}, M. Casarsa^a, F. Cossutti^a, A. Da Rold^{a,b}, G. Della Ricca^{a,b}, F. Vazzoler^{a,b}, A. Zanetti^a

Kyungpook National University, Daegu, Korea

B. Kim, D.H. Kim, G.N. Kim, J. Lee, S.W. Lee, C.S. Moon, Y.D. Oh, S.I. Pak, S. Sekmen, D.C. Son, Y.C. Yang

Chonnam National University, Institute for Universe and Elementary Particles, Kwangju, Korea

H. Kim, D.H. Moon, G. Oh

Hanyang University, Seoul, Korea

B. Francois, T.J. Kim, J. Park

Korea University, Seoul, Korea

S. Cho, S. Choi, Y. Go, S. Ha, B. Hong, K. Lee, K.S. Lee, J. Lim, J. Park, S.K. Park, Y. Roh, J. Yoo

Kyung Hee University, Department of Physics

J. Goh

Sejong University, Seoul, Korea

H.S. Kim

Seoul National University, Seoul, Korea

J. Almond, J.H. Bhyun, J. Choi, S. Jeon, J. Kim, J.S. Kim, H. Lee, K. Lee, S. Lee, K. Nam, M. Oh, S.B. Oh, B.C. Radburn-Smith, U.K. Yang, H.D. Yoo, I. Yoon

University of Seoul, Seoul, Korea

D. Jeon, H. Kim, J.H. Kim, J.S.H. Lee, I.C. Park, I.J. Watson

Sungkyunkwan University, Suwon, Korea

Y. Choi, C. Hwang, Y. Jeong, J. Lee, Y. Lee, I. Yu

Riga Technical University, Riga, Latvia

V. Veckalns³³

Vilnius University, Vilnius, Lithuania

V. Dudenas, A. Juodagalvis, A. Rinkevicius, G. Tamulaitis, J. Vaitkus

National Centre for Particle Physics, Universiti Malaya, Kuala Lumpur, Malaysia

Z.A. Ibrahim, F. Mohamad Idris³⁴, W.A.T. Wan Abdullah, M.N. Yusli, Z. Zolkapli

Universidad de Sonora (UNISON), Hermosillo, Mexico

J.F. Benitez, A. Castaneda Hernandez, J.A. Murillo Quijada, L. Valencia Palomo

Centro de Investigacion y de Estudios Avanzados del IPN, Mexico City, Mexico

H. Castilla-Valdez, E. De La Cruz-Burelo, I. Heredia-De La Cruz³⁵, R. Lopez-Fernandez, A. Sanchez-Hernandez

Universidad Iberoamericana, Mexico City, Mexico

S. Carrillo Moreno, C. Oropeza Barrera, M. Ramirez-Garcia, F. Vazquez Valencia

Benemerita Universidad Autonoma de Puebla, Puebla, Mexico

J. Eysermans, I. Pedraza, H.A. Salazar Ibarguen, C. Uribe Estrada

Universidad Autónoma de San Luis Potosí, San Luis Potosí, Mexico

A. Morelos Pineda

University of Montenegro, Podgorica, Montenegro

J. Mijuskovic², N. Raicevic

University of Auckland, Auckland, New Zealand

D. Krofcheck

University of Canterbury, Christchurch, New Zealand

S. Bheesette, P.H. Butler

National Centre for Physics, Quaid-I-Azam University, Islamabad, Pakistan

A. Ahmad, M. Ahmad, Q. Hassan, H.R. Hoorani, W.A. Khan, M.A. Shah, M. Shoaib, M. Waqas

AGH University of Science and Technology Faculty of Computer Science, Electronics and Telecommunications, Krakow, Poland

V. Avati, L. Grzanka, M. Malawski

National Centre for Nuclear Research, Swierk, Poland

H. Bialkowska, M. Bluj, B. Boimska, M. Górski, M. Kazana, M. Szeleper, P. Zalewski

Institute of Experimental Physics, Faculty of Physics, University of Warsaw, Warsaw, Poland

K. Bunkowski, A. Byszuk³⁶, K. Doroba, A. Kalinowski, M. Konecki, J. Krolikowski, M. Misiura, M. Olszewski, M. Walczak

Laboratório de Instrumentação e Física Experimental de Partículas, Lisboa, Portugal

M. Araujo, P. Bargassa, D. Bastos, A. Di Francesco, P. Faccioli, B. Galinhas, M. Gallinaro, J. Hollar, N. Leonardo, T. Niknejad, J. Seixas, K. Shchelina, G. Strong, O. Toldaiev, J. Varela

Joint Institute for Nuclear Research, Dubna, Russia

S. Afanasiev, P. Bunin, M. Gavrilenko, I. Golutvin, I. Gorbunov, A. Kamenev, V. Karjavine, A. Lanev, A. Malakhov, V. Matveev^{37,38}, P. Moiseenz, V. Palichik, V. Perelygin, M. Savina, S. Shmatov, S. Shulha, N. Skatchkov, V. Smirnov, N. Voytishin, A. Zarubin

Petersburg Nuclear Physics Institute, Gatchina (St. Petersburg), Russia

L. Chtchipounov, V. Golovtcov, Y. Ivanov, V. Kim³⁹, E. Kuznetsova⁴⁰, P. Levchenko, V. Murzin, V. Oreshkin, I. Smirnov, D. Sosnov, V. Sulimov, L. Uvarov, A. Vorobyev

Institute for Nuclear Research, Moscow, Russia

Yu. Andreev, A. Dermenev, S. Gninenko, N. Golubev, A. Karneyeu, M. Kirsanov, N. Krasnikov, A. Pashenkov, D. Tlisov, A. Toropin

Institute for Theoretical and Experimental Physics named by A.I. Alikhanov of NRC 'Kurchatov Institute', Moscow, Russia

V. Epshteyn, V. Gavrilov, N. Lychkovskaya, A. Nikitenko⁴¹, V. Popov, I. Pozdnyakov, G. Safronov, A. Spiridonov, A. Stepenov, M. Toms, E. Vlasov, A. Zhokin

Moscow Institute of Physics and Technology, Moscow, Russia

T. Aushev

National Research Nuclear University 'Moscow Engineering Physics Institute' (MEPhI), Moscow, Russia

M. Chadeeva⁴², P. Parygin, D. Philippov, E. Popova, V. Rusinov

P.N. Lebedev Physical Institute, Moscow, Russia

V. Andreev, M. Azarkin, I. Dremin, M. Kirakosyan, A. Terkulov

Skobeltsyn Institute of Nuclear Physics, Lomonosov Moscow State University, Moscow, Russia

A. Baskakov, A. Belyaev, E. Boos, V. Bunichev, M. Dubinin⁴³, L. Dudko, A. Gribushin, V. Klyukhin, I. Lokhtin, S. Obraztsov, M. Perfilov, S. Petrushanko, V. Savrin

Novosibirsk State University (NSU), Novosibirsk, Russia

A. Barnyakov⁴⁴, V. Blinov⁴⁴, T. Dimova⁴⁴, L. Kardapol'tsev⁴⁴, Y. Skovpen⁴⁴

Institute for High Energy Physics of National Research Centre 'Kurchatov Institute', Protvino, Russia

I. Azhgirey, I. Bayshev, S. Bitioukov, V. Kachanov, D. Konstantinov, P. Mandrik, V. Petrov, R. Ryutin, S. Slabospitskii, A. Sobol, S. Troshin, N. Tyurin, A. Uzunian, A. Volkov

National Research Tomsk Polytechnic University, Tomsk, Russia

A. Babaev, A. Iuzhakov, V. Okhotnikov

Tomsk State University, Tomsk, Russia

V. Borchsh, V. Ivanchenko, E. Tcherniaev

University of Belgrade: Faculty of Physics and VINCA Institute of Nuclear Sciences

P. Adzic⁴⁵, P. Cirkovic, M. Dordevic, P. Milenovic, J. Milosevic, M. Stojanovic

Centro de Investigaciones Energéticas Medioambientales y Tecnológicas (CIEMAT), Madrid, Spain

M. Aguilar-Benitez, J. Alcaraz Maestre, A. Alvarez Fernández, I. Bachiller, M. Barrio Luna, Cristina F. Bedoya, J.A. Brochero Cifuentes, C.A. Carrillo Montoya, M. Cepeda, M. Cerrada, N. Colino, B. De La Cruz, A. Delgado Peris, J.P. Fernández Ramos, J. Flix, M.C. Fouz, O. Gonzalez Lopez, S. Goy Lopez, J.M. Hernandez, M.I. Josa, D. Moran, . Navarro Tobar, A. Pérez-Calero Yzquierdo, J. Puerta Pelayo, I. Redondo, L. Romero, S. Sánchez Navas, M.S. Soares, A. Triossi, C. Willmott

Universidad Autónoma de Madrid, Madrid, Spain

C. Albajar, J.F. de Trocóniz, R. Reyes-Almanza

Universidad de Oviedo, Instituto Universitario de Ciencias y Tecnologías Espaciales de Asturias (ICTEA), Oviedo, Spain

B. Alvarez Gonzalez, J. Cuevas, C. Erice, J. Fernandez Menendez, S. Folgueras, I. Gonzalez Caballero, J.R. González Fernández, E. Palencia Cortezon, V. Rodríguez Bouza, S. Sanchez Cruz

Instituto de Física de Cantabria (IFCA), CSIC-Universidad de Cantabria, Santander, Spain

I.J. Cabrillo, A. Calderon, B. Chazin Quero, J. Duarte Campderros, M. Fernandez,

P.J. Fernández Manteca, A. García Alonso, G. Gomez, C. Martinez Rivero, P. Martinez Ruiz del Arbol, F. Matorras, J. Piedra Gomez, C. Prieels, T. Rodrigo, A. Ruiz-Jimeno, L. Russo⁴⁶, L. Scodellaro, I. Vila, J.M. Vizan Garcia

University of Colombo, Colombo, Sri Lanka

K. Malagalage

University of Ruhuna, Department of Physics, Matara, Sri Lanka

W.G.D. Dharmaratna, N. Wickramage

CERN, European Organization for Nuclear Research, Geneva, Switzerland

D. Abbaneo, B. Akgun, E. Auffray, G. Auzinger, J. Baechler, P. Baillon, A.H. Ball, D. Barney, J. Bendavid, M. Bianco, A. Bocci, P. Bortignon, E. Bossini, C. Botta, E. Brondolin, T. Camporesi, A. Caratelli, G. Cerminara, E. Chapon, G. Cucciati, D. d'Enterria, A. Dabrowski, N. Daci, V. Daponte, A. David, O. Davignon, A. De Roeck, M. Deile, M. Dobson, M. Dünser, N. Dupont, A. Elliott-Peisert, N. Emriskova, F. Fallavollita⁴⁷, D. Fasanella, S. Fiorendi, G. Franzoni, J. Fulcher, W. Funk, S. Giani, D. Gigi, A. Gilbert, K. Gill, F. Glege, L. Gouskos, M. Gruchala, M. Guilbaud, D. Gulhan, J. Hegeman, C. Heidegger, Y. Iiyama, V. Innocente, T. James, P. Janot, O. Karacheban¹⁹, J. Kaspar, J. Kieseler, M. Krammer¹, N. Kratochwil, C. Lange, P. Lecoq, C. Lourenço, L. Malgeri, M. Mannelli, A. Massironi, F. Meijers, J.A. Merlin, S. Mersi, E. Meschi, F. Moortgat, M. Mulders, J. Ngadiuba, J. Niedziela, S. Nourbakhsh, S. Orfanelli, L. Orsini, F. Pantaleo¹⁶, L. Pape, E. Perez, M. Peruzzi, A. Petrilli, G. Petrucciani, A. Pfeiffer, M. Pierini, F.M. Pitters, D. Rabady, A. Racz, M. Rieger, M. Rovere, H. Sakulin, C. Schäfer, C. Schwick, M. Selvaggi, A. Sharma, P. Silva, W. Snoeys, P. Sphicas⁴⁸, J. Steggemann, S. Summers, V.R. Tavolaro, D. Treille, A. Tsirou, G.P. Van Onsem, A. Vartak, M. Verzetti, W.D. Zeuner

Paul Scherrer Institut, Villigen, Switzerland

L. Caminada⁴⁹, K. Deiters, W. Erdmann, R. Horisberger, Q. Ingram, H.C. Kaestli, D. Kotlinski, U. Langenegger, T. Rohe, S.A. Wiederkehr

ETH Zurich - Institute for Particle Physics and Astrophysics (IPA), Zurich, Switzerland

M. Backhaus, P. Berger, N. Chernyavskaya, G. Dissertori, M. Dittmar, M. Donegà, C. Dorfer, T.A. Gómez Espinosa, C. Grab, D. Hits, W. Lustermann, R.A. Manzoni, M.T. Meinhard, F. Micheli, P. Musella, F. Nessi-Tedaldi, F. Pauss, G. Perrin, L. Perrozzi, S. Pigazzini, M.G. Ratti, M. Reichmann, C. Reissel, T. Reitenspiess, B. Ristic, D. Ruini, D.A. Sanz Becerra, M. Schönenberger, L. Shchutska, M.L. Vesterbacka Olsson, R. Wallny, D.H. Zhu

Universität Zürich, Zurich, Switzerland

T.K. Aarrestad, C. AMSler⁵⁰, D. Brzhechko, M.F. Canelli, A. De Cosa, R. Del Burgo, B. Kilminster, S. Leontsinis, V.M. Mikuni, I. Neutelings, G. Rauco, P. Robmann, K. Schweiger, C. Seitz, Y. Takahashi, S. Wertz, A. Zucchetta

National Central University, Chung-Li, Taiwan

T.H. Doan, C.M. Kuo, W. Lin, A. Roy, S.S. Yu

National Taiwan University (NTU), Taipei, Taiwan

P. Chang, Y. Chao, K.F. Chen, P.H. Chen, W.-S. Hou, Y.y. Li, R.-S. Lu, E. Paganis, A. Psallidas, A. Steen

Chulalongkorn University, Faculty of Science, Department of Physics, Bangkok, Thailand

B. Asavapibhop, C. Asawatangtrakuldee, N. Srimanobhas, N. Suwonjandee

ukurova University, Physics Department, Science and Art Faculty, Adana, Turkey

A. Bat, F. Boran, A. Celik⁵¹, S. Cerci⁵², S. Damarseckin⁵³, Z.S. Demiroglu, F. Dolek, C. Dozen⁵⁴,

I. Dumanoglu, G. Gokbulut, EmineGurpinar Guler⁵⁵, Y. Guler, I. Hos⁵⁶, C. Isik, E.E. Kangal⁵⁷, O. Kara, A. Kayis Topaksu, U. Kiminsu, G. Onengut, K. Ozdemir⁵⁸, S. Ozturk⁵⁹, A.E. Simsek, D. Sunar Cerci⁵², U.G. Tok, S. Turkcapar, I.S. Zorbakir, C. Zorbilmez

Middle East Technical University, Physics Department, Ankara, Turkey

B. Isildak⁶⁰, G. Karapinar⁶¹, M. Yalvac

Bogazici University, Istanbul, Turkey

I.O. Atakisi, E. Gülmez, M. Kaya⁶², O. Kaya⁶³, Ö. Özçelik, S. Tekten, E.A. Yetkin⁶⁴

Istanbul Technical University, Istanbul, Turkey

A. Cakir, K. Cankocak, Y. Komurcu, S. Sen⁶⁵

Istanbul University, Istanbul, Turkey

B. Kaynak, S. Ozkorucuklu

Institute for Scintillation Materials of National Academy of Science of Ukraine, Kharkov, Ukraine

B. Grynyov

National Scientific Center, Kharkov Institute of Physics and Technology, Kharkov, Ukraine

L. Levchuk

University of Bristol, Bristol, United Kingdom

E. Bhal, S. Bologna, J.J. Brooke, D. Burns⁶⁶, E. Clement, D. Cussans, H. Flacher, J. Goldstein, G.P. Heath, H.F. Heath, L. Kreczko, B. Krikler, S. Paramesvaran, B. Penning, T. Sakuma, S. Seif El Nasr-Storey, V.J. Smith, J. Taylor, A. Titterton

Rutherford Appleton Laboratory, Didcot, United Kingdom

K.W. Bell, A. Belyaev⁶⁷, C. Brew, R.M. Brown, D.J.A. Cockerill, J.A. Coughlan, K. Harder, S. Harper, J. Linacre, K. Manolopoulos, D.M. Newbold, E. Olaiya, D. Petyt, T. Reis, T. Schuh, C.H. Shepherd-Themistocleous, A. Thea, I.R. Tomalin, T. Williams, W.J. Womersley

Imperial College, London, United Kingdom

R. Bainbridge, P. Bloch, J. Borg, S. Breeze, O. Buchmuller, A. Bundock, GurpreetSingh CHAHAL⁶⁸, D. Colling, P. Dauncey, G. Davies, M. Della Negra, R. Di Maria, P. Everaerts, G. Hall, G. Iles, M. Komm, C. Laner, L. Lyons, A.-M. Magnan, S. Malik, A. Martelli, V. Milosevic, A. Morton, J. Nash⁶⁹, V. Palladino, M. Pesaresi, D.M. Raymond, A. Richards, A. Rose, E. Scott, C. Seez, A. Shtipliyski, M. Stoye, T. Strebler, A. Tapper, K. Uchida, T. Virdee¹⁶, N. Wardle, D. Winterbottom, J. Wright, A.G. Zecchinelli, S.C. Zenz

Brunel University, Uxbridge, United Kingdom

J.E. Cole, P.R. Hobson, A. Khan, P. Kyberd, C.K. Mackay, I.D. Reid, L. Teodorescu, S. Zahid

Baylor University, Waco, USA

K. Call, B. Caraway, J. Dittmann, K. Hatakeyama, C. Madrid, B. McMaster, N. Pastika, C. Smith

Catholic University of America, Washington, DC, USA

R. Bartek, A. Dominguez, R. Uniyal, A.M. Vargas Hernandez

The University of Alabama, Tuscaloosa, USA

A. Buccilli, S.I. Cooper, C. Henderson, P. Rumerio, C. West

Boston University, Boston, USA

A. Albert, D. Arcaro, Z. Demiragli, D. Gastler, C. Richardson, J. Rohlf, D. Sperka, I. Suarez, L. Sulak, D. Zou

Brown University, Providence, USA

G. Benelli, B. Burkler, X. Coubez¹⁷, D. Cutts, Y.t. Duh, M. Hadley, U. Heintz, J.M. Hogan⁷⁰, K.H.M. Kwok, E. Laird, G. Landsberg, K.T. Lau, J. Lee, Z. Mao, M. Narain, S. Sagir⁷¹, R. Syarif, E. Usai, D. Yu, W. Zhang

University of California, Davis, Davis, USA

R. Band, C. Brainerd, R. Breedon, M. Calderon De La Barca Sanchez, M. Chertok, J. Conway, R. Conway, P.T. Cox, R. Erbacher, C. Flores, G. Funk, F. Jensen, W. Ko, O. Kukral, R. Lander, M. Mulhearn, D. Pellett, J. Pilot, M. Shi, D. Taylor, K. Tos, M. Tripathi, Z. Wang, F. Zhang

University of California, Los Angeles, USA

M. Bachtis, C. Bravo, R. Cousins, A. Dasgupta, A. Florent, J. Hauser, M. Ignatenko, N. Mccoll, W.A. Nash, S. Regnard, D. Saltzberg, C. Schnaible, B. Stone, V. Valuev

University of California, Riverside, Riverside, USA

K. Burt, Y. Chen, R. Clare, J.W. Gary, S.M.A. Ghiasi Shirazi, G. Hanson, G. Karapostoli, E. Kennedy, O.R. Long, M. Olmedo Negrete, M.I. Paneva, W. Si, L. Wang, S. Wimpenny, B.R. Yates, Y. Zhang

University of California, San Diego, La Jolla, USA

J.G. Branson, P. Chang, S. Cittolin, S. Cooperstein, N. Deelen, M. Derdzinski, R. Gerosa, D. Gilbert, B. Hashemi, D. Klein, V. Krutelyov, J. Letts, M. Masciovecchio, S. May, S. Padhi, M. Pieri, V. Sharma, M. Tadel, F. Würthwein, A. Yagil, G. Zevi Della Porta

University of California, Santa Barbara - Department of Physics, Santa Barbara, USA

N. Amin, R. Bhandari, C. Campagnari, M. Citron, V. Dutta, M. Franco Sevilla, J. Incandela, B. Marsh, H. Mei, A. Ovcharova, H. Qu, J. Richman, U. Sarica, D. Stuart, S. Wang

California Institute of Technology, Pasadena, USA

D. Anderson, A. Bornheim, O. Cerri, I. Dutta, J.M. Lawhorn, N. Lu, J. Mao, H.B. Newman, T.Q. Nguyen, J. Pata, M. Spiropulu, J.R. Vlimant, S. Xie, Z. Zhang, R.Y. Zhu

Carnegie Mellon University, Pittsburgh, USA

M.B. Andrews, T. Ferguson, T. Mudholkar, M. Paulini, M. Sun, I. Vorobiev, M. Weinberg

University of Colorado Boulder, Boulder, USA

J.P. Cumalat, W.T. Ford, E. MacDonald, T. Mulholland, R. Patel, A. Perloff, K. Stenson, K.A. Ulmer, S.R. Wagner

Cornell University, Ithaca, USA

J. Alexander, Y. Cheng, J. Chu, A. Datta, A. Frankenthal, K. Mcdermott, J.R. Patterson, D. Quach, A. Ryd, S.M. Tan, Z. Tao, J. Thom, P. Wittich, M. Zientek

Fermi National Accelerator Laboratory, Batavia, USA

S. Abdullin, M. Albrow, M. Alyari, G. Apollinari, A. Apresyan, A. Apyan, S. Banerjee, L.A.T. Bauerdick, A. Beretvas, D. Berry, J. Berryhill, P.C. Bhat, K. Burkett, J.N. Butler, A. Canepa, G.B. Cerati, H.W.K. Cheung, F. Chlebana, M. Cremonesi, J. Duarte, V.D. Elvira, J. Freeman, Z. Gecse, E. Gottschalk, L. Gray, D. Green, S. Grünendahl, O. Gutsche, AllisonReinsvold Hall, J. Hanlon, R.M. Harris, S. Hasegawa, R. Heller, J. Hirschauer, B. Jayatilaka, S. Jindariani, M. Johnson, U. Joshi, T. Klijnsma, B. Klima, M.J. Kortelainen, B. Kreis, S. Lammel, J. Lewis, D. Lincoln, R. Lipton, M. Liu, T. Liu, J. Lykken, K. Maeshima, J.M. Marraffino, D. Mason, P. McBride, P. Merkel, S. Mrenna, S. Nahn, V. O'Dell, V. Papadimitriou, K. Pedro, C. Pena, G. Rakness, F. Ravera, L. Ristori, B. Schneider, E. Sexton-Kennedy, N. Smith, A. Soha,

W.J. Spalding, L. Spiegel, S. Stoynev, J. Strait, N. Strobbe, L. Taylor, S. Tkaczyk, N.V. Tran, L. Uplegger, E.W. Vaandering, C. Vernieri, R. Vidal, M. Wang, H.A. Weber

University of Florida, Gainesville, USA

D. Acosta, P. Avery, D. Bourilkov, A. Brinkerhoff, L. Cadamuro, A. Carnes, V. Cherepanov, F. Errico, R.D. Field, S.V. Gleyzer, B.M. Joshi, M. Kim, J. Konigsberg, A. Korytov, K.H. Lo, P. Ma, K. Matchev, N. Menendez, G. Mitselmakher, D. Rosenzweig, K. Shi, J. Wang, S. Wang, X. Zuo

Florida International University, Miami, USA

Y.R. Joshi

Florida State University, Tallahassee, USA

T. Adams, A. Askew, S. Hagopian, V. Hagopian, K.F. Johnson, R. Khurana, T. Kolberg, G. Martinez, T. Perry, H. Prosper, C. Schiber, R. Yohay, J. Zhang

Florida Institute of Technology, Melbourne, USA

M.M. Baarmand, M. Hohlmann, D. Noonan, M. Rahmani, M. Saunders, F. Yumiceva

University of Illinois at Chicago (UIC), Chicago, USA

M.R. Adams, L. Apanasevich, R.R. Betts, R. Cavanaugh, X. Chen, S. Dittmer, O. Evdokimov, C.E. Gerber, D.A. Hangal, D.J. Hofman, K. Jung, C. Mills, T. Roy, M.B. Tonjes, N. Varelas, J. Viinikainen, H. Wang, X. Wang, Z. Wu

The University of Iowa, Iowa City, USA

M. Alhusseini, B. Bilki⁵⁵, W. Clarida, K. Dilsiz⁷², S. Durgut, R.P. Gandrajula, M. Haytmyradov, V. Khristenko, O.K. Köseyan, J.-P. Merlo, A. Mestvirishvili⁷³, A. Moeller, J. Nachtman, H. Ogul⁷⁴, Y. Onel, F. Ozok⁷⁵, A. Penzo, C. Snyder, E. Tiras, J. Wetzel

Johns Hopkins University, Baltimore, USA

B. Blumenfeld, A. Cocoros, N. Eminizer, A.V. Gritsan, W.T. Hung, S. Kyriacou, P. Maksimovic, J. Roskes, M. Swartz

The University of Kansas, Lawrence, USA

C. Baldenegro Barrera, P. Baringer, A. Bean, S. Boren, J. Bowen, A. Bylinkin, T. Isidori, S. Khalil, J. King, G. Krintiras, A. Kropivnitskaya, C. Lindsey, D. Majumder, W. Mcbrayer, N. Minafra, M. Murray, C. Rogan, C. Royon, S. Sanders, E. Schmitz, J.D. Tapia Takaki, Q. Wang, J. Williams, G. Wilson

Kansas State University, Manhattan, USA

S. Duric, A. Ivanov, K. Kaadze, D. Kim, Y. Maravin, D.R. Mendis, T. Mitchell, A. Modak, A. Mohammadi

Lawrence Livermore National Laboratory, Livermore, USA

F. Rebassoo, D. Wright

University of Maryland, College Park, USA

A. Baden, O. Baron, A. Belloni, S.C. Eno, Y. Feng, N.J. Hadley, S. Jabeen, G.Y. Jeng, R.G. Kellogg, J. Kunkle, A.C. Mignerey, S. Nabili, F. Ricci-Tam, M. Seidel, Y.H. Shin, A. Skuja, S.C. Tonwar, K. Wong

Massachusetts Institute of Technology, Cambridge, USA

D. Abercrombie, B. Allen, A. Baty, R. Bi, S. Brandt, W. Busza, I.A. Cali, M. D'Alfonso, G. Gomez Ceballos, M. Goncharov, P. Harris, D. Hsu, M. Hu, M. Klute, D. Kovalskyi, Y.-J. Lee, P.D. Luckey, B. Maier, A.C. Marini, C. Mcginn, C. Mironov, S. Narayanan, X. Niu, C. Paus,

D. Rankin, C. Roland, G. Roland, Z. Shi, G.S.F. Stephans, K. Sumorok, K. Tatar, D. Velicanu, J. Wang, T.W. Wang, B. Wyslouch

University of Minnesota, Minneapolis, USA

R.M. Chatterjee, A. Evans, S. Guts[†], P. Hansen, J. Hiltbrand, Sh. Jain, Y. Kubota, Z. Lesko, J. Mans, M. Revering, R. Rusack, R. Saradhy, N. Schroeder, M.A. Wadud

University of Mississippi, Oxford, USA

J.G. Acosta, S. Oliveros

University of Nebraska-Lincoln, Lincoln, USA

K. Bloom, S. Chauhan, D.R. Claes, C. Fangmeier, L. Finco, F. Golf, R. Kamalieddin, I. Kravchenko, J.E. Siado, G.R. Snow[†], B. Stieger, W. Tabb

State University of New York at Buffalo, Buffalo, USA

G. Agarwal, C. Harrington, I. Iashvili, A. Kharchilava, C. McLean, D. Nguyen, A. Parker, J. Pekkanen, S. Rappoccio, B. Roozbahani

Northeastern University, Boston, USA

G. Alverson, E. Barberis, C. Freer, Y. Haddad, A. Hortiangtham, G. Madigan, B. Marzocchi, D.M. Morse, T. Orimoto, L. Skinnari, A. Tishelman-Charny, T. Wamorkar, B. Wang, A. Wisecarver, D. Wood

Northwestern University, Evanston, USA

S. Bhattacharya, J. Bueghly, T. Gunter, K.A. Hahn, N. Odell, M.H. Schmitt, K. Sung, M. Trovato, M. Velasco

University of Notre Dame, Notre Dame, USA

R. Bucci, N. Dev, R. Goldouzian, M. Hildreth, K. Hurtado Anampa, C. Jessop, D.J. Karmgard, K. Lannon, W. Li, N. Loukas, N. Marinelli, I. Mcalister, F. Meng, C. Mueller, Y. Musienko³⁷, M. Planer, R. Ruchti, P. Siddireddy, G. Smith, S. Taroni, M. Wayne, A. Wightman, M. Wolf, A. Woodard

The Ohio State University, Columbus, USA

J. Alimena, B. Bylsma, L.S. Durkin, B. Francis, C. Hill, W. Ji, A. Lefeld, T.Y. Ling, B.L. Winer

Princeton University, Princeton, USA

G. Dezoort, P. Elmer, J. Hardenbrook, N. Haubrich, S. Higginbotham, A. Kalogeropoulos, S. Kwan, D. Lange, M.T. Lucchini, J. Luo, D. Marlow, K. Mei, I. Ojalvo, J. Olsen, C. Palmer, P. Piroué, J. Salfeld-Nebgen, D. Stickland, C. Tully, Z. Wang

University of Puerto Rico, Mayaguez, USA

S. Malik, S. Norberg

Purdue University, West Lafayette, USA

A. Barker, V.E. Barnes, S. Das, L. Gutay, M. Jones, A.W. Jung, A. Khatiwada, B. Mahakud, D.H. Miller, G. Negro, N. Neumeister, C.C. Peng, S. Piperov, H. Qiu, J.F. Schulte, N. Trevisani, F. Wang, R. Xiao, W. Xie

Purdue University Northwest, Hammond, USA

T. Cheng, J. Dolen, N. Parashar

Rice University, Houston, USA

U. Behrens, K.M. Ecklund, S. Freed, F.J.M. Geurts, M. Kilpatrick, Arun Kumar, W. Li, B.P. Padley, R. Redjimi, J. Roberts, J. Rorie, W. Shi, A.G. Stahl Leiton, Z. Tu, A. Zhang

University of Rochester, Rochester, USA

A. Bodek, P. de Barbaro, R. Demina, J.L. Dulemba, C. Fallon, T. Ferbel, M. Galanti, A. Garcia-Bellido, O. Hindrichs, A. Khukhunaishvili, E. Ranken, R. Taus

Rutgers, The State University of New Jersey, Piscataway, USA

B. Chiarito, J.P. Chou, A. Gandrakota, Y. Gershtein, E. Halkiadakis, A. Hart, M. Heindl, E. Hughes, S. Kaplan, I. Laflotte, A. Lath, R. Montalvo, K. Nash, M. Osherson, H. Saka, S. Salur, S. Schnetzer, S. Somalwar, R. Stone, S. Thomas

University of Tennessee, Knoxville, USA

H. Acharya, A.G. Delannoy, S. Spanier

Texas A&M University, College Station, USA

O. Bouhali⁷⁶, M. Dalchenko, M. De Mattia, A. Delgado, S. Dildick, R. Eusebi, J. Gilmore, T. Huang, T. Kamon⁷⁷, S. Luo, S. Malhotra, D. Marley, R. Mueller, D. Overton, L. Perniè, D. Rathjens, A. Safonov

Texas Tech University, Lubbock, USA

N. Akchurin, J. Damgov, F. De Guio, S. Kunori, K. Lamichhane, S.W. Lee, T. Mengke, S. Muthumuni, T. Peltola, S. Undleeb, I. Volobouev, Z. Wang, A. Whitbeck

Vanderbilt University, Nashville, USA

S. Greene, A. Gurrola, R. Janjam, W. Johns, C. Maguire, A. Melo, H. Ni, K. Padeken, F. Romeo, P. Sheldon, S. Tuo, J. Velkovska, M. Verweij

University of Virginia, Charlottesville, USA

M.W. Arenton, P. Barria, B. Cox, G. Cummings, J. Hakala, R. Hirosky, M. Joyce, A. Ledovskoy, C. Neu, B. Tannenwald, Y. Wang, E. Wolfe, F. Xia

Wayne State University, Detroit, USA

R. Harr, P.E. Karchin, N. Poudyal, J. Sturdy, P. Thapa

University of Wisconsin - Madison, Madison, WI, USA

T. Bose, J. Buchanan, C. Caillol, D. Carlsmith, S. Dasu, I. De Bruyn, L. Dodd, F. Fiori, C. Galloni, H. He, M. Herndon, A. Hervé, U. Hussain, P. Klabbers, A. Lanaro, A. Loeliger, K. Long, R. Loveless, J. Madhusudanan Sreekala, D. Pinna, T. Ruggles, A. Savin, V. Sharma, W.H. Smith, D. Teague, S. Trembath-reichert, N. Woods

†: Deceased

1: Also at Vienna University of Technology, Vienna, Austria

2: Also at IRFU, CEA, Université Paris-Saclay, Gif-sur-Yvette, France

3: Also at Universidade Estadual de Campinas, Campinas, Brazil

4: Also at Federal University of Rio Grande do Sul, Porto Alegre, Brazil

5: Also at UFMS, Nova Andradina, Brazil

6: Also at Universidade Federal de Pelotas, Pelotas, Brazil

7: Also at Université Libre de Bruxelles, Bruxelles, Belgium

8: Also at University of Chinese Academy of Sciences, Beijing, China

9: Also at Institute for Theoretical and Experimental Physics named by A.I. Alikhanov of NRC 'Kurchatov Institute', Moscow, Russia

10: Also at Joint Institute for Nuclear Research, Dubna, Russia

11: Also at Cairo University, Cairo, Egypt

12: Also at Zewail City of Science and Technology, Zewail, Egypt

13: Also at Purdue University, West Lafayette, USA

14: Also at Université de Haute Alsace, Mulhouse, France

- 15: Also at Erzincan Binali Yildirim University, Erzincan, Turkey
- 16: Also at CERN, European Organization for Nuclear Research, Geneva, Switzerland
- 17: Also at RWTH Aachen University, III. Physikalisches Institut A, Aachen, Germany
- 18: Also at University of Hamburg, Hamburg, Germany
- 19: Also at Brandenburg University of Technology, Cottbus, Germany
- 20: Also at Institute of Physics, University of Debrecen, Debrecen, Hungary, Debrecen, Hungary
- 21: Also at Institute of Nuclear Research ATOMKI, Debrecen, Hungary
- 22: Also at MTA-ELTE Lendület CMS Particle and Nuclear Physics Group, Eötvös Loránd University, Budapest, Hungary, Budapest, Hungary
- 23: Also at IIT Bhubaneswar, Bhubaneswar, India, Bhubaneswar, India
- 24: Also at Institute of Physics, Bhubaneswar, India
- 25: Also at Shoolini University, Solan, India
- 26: Also at University of Hyderabad, Hyderabad, India
- 27: Also at University of Visva-Bharati, Santiniketan, India
- 28: Also at Isfahan University of Technology, Isfahan, Iran
- 29: Now at INFN Sezione di Bari ^a, Università di Bari ^b, Politecnico di Bari ^c, Bari, Italy
- 30: Also at Italian National Agency for New Technologies, Energy and Sustainable Economic Development, Bologna, Italy
- 31: Also at Centro Siciliano di Fisica Nucleare e di Struttura Della Materia, Catania, Italy
- 32: Also at Scuola Normale e Sezione dell'INFN, Pisa, Italy
- 33: Also at Riga Technical University, Riga, Latvia, Riga, Latvia
- 34: Also at Malaysian Nuclear Agency, MOSTI, Kajang, Malaysia
- 35: Also at Consejo Nacional de Ciencia y Tecnología, Mexico City, Mexico
- 36: Also at Warsaw University of Technology, Institute of Electronic Systems, Warsaw, Poland
- 37: Also at Institute for Nuclear Research, Moscow, Russia
- 38: Now at National Research Nuclear University 'Moscow Engineering Physics Institute' (MEPhI), Moscow, Russia
- 39: Also at St. Petersburg State Polytechnical University, St. Petersburg, Russia
- 40: Also at University of Florida, Gainesville, USA
- 41: Also at Imperial College, London, United Kingdom
- 42: Also at P.N. Lebedev Physical Institute, Moscow, Russia
- 43: Also at California Institute of Technology, Pasadena, USA
- 44: Also at Budker Institute of Nuclear Physics, Novosibirsk, Russia
- 45: Also at Faculty of Physics, University of Belgrade, Belgrade, Serbia
- 46: Also at Università degli Studi di Siena, Siena, Italy
- 47: Also at INFN Sezione di Pavia ^a, Università di Pavia ^b, Pavia, Italy, Pavia, Italy
- 48: Also at National and Kapodistrian University of Athens, Athens, Greece
- 49: Also at Universität Zürich, Zurich, Switzerland
- 50: Also at Stefan Meyer Institute for Subatomic Physics, Vienna, Austria, Vienna, Austria
- 51: Also at Burdur Mehmet Akif Ersoy University, BURDUR, Turkey
- 52: Also at Adiyaman University, Adiyaman, Turkey
- 53: Also at Şırnak University, Sırnak, Turkey
- 54: Also at Tsinghua University, Beijing, China
- 55: Also at Beykent University, Istanbul, Turkey, Istanbul, Turkey
- 56: Also at Istanbul Aydın University, Application and Research Center for Advanced Studies (App. & Res. Cent. for Advanced Studies), Istanbul, Turkey
- 57: Also at Mersin University, Mersin, Turkey
- 58: Also at Piri Reis University, Istanbul, Turkey

- 59: Also at Gaziosmanpasa University, Tokat, Turkey
- 60: Also at Ozyegin University, Istanbul, Turkey
- 61: Also at Izmir Institute of Technology, Izmir, Turkey
- 62: Also at Marmara University, Istanbul, Turkey
- 63: Also at Kafkas University, Kars, Turkey
- 64: Also at Istanbul Bilgi University, Istanbul, Turkey
- 65: Also at Hacettepe University, Ankara, Turkey
- 66: Also at Vrije Universiteit Brussel, Brussel, Belgium
- 67: Also at School of Physics and Astronomy, University of Southampton, Southampton, United Kingdom
- 68: Also at IPPP Durham University, Durham, United Kingdom
- 69: Also at Monash University, Faculty of Science, Clayton, Australia
- 70: Also at Bethel University, St. Paul, Minneapolis, USA, St. Paul, USA
- 71: Also at Karamanoğlu Mehmetbey University, Karaman, Turkey
- 72: Also at Bingol University, Bingol, Turkey
- 73: Also at Georgian Technical University, Tbilisi, Georgia
- 74: Also at Sinop University, Sinop, Turkey
- 75: Also at Mimar Sinan University, Istanbul, Istanbul, Turkey
- 76: Also at Texas A&M University at Qatar, Doha, Qatar
- 77: Also at Kyungpook National University, Daegu, Korea, Daegu, Korea